Zeb2 is essential for Schwann cell differentiation, myelination and nerve repair

Sip1 is essential for Schwann cell differentiation, myelination and nerve repair

Susanne Quintes[1,2,*], Bastian G. Brinkmann[1,*], Madlen Ebert[1], Franziska Fröb[3], Theresa Kungl[1], Friederike A. Arlt[1], Victor Tarabykin[4], Danny Huylebroeck[5], Dies Meijer[6], Ueli Suter[7], Michael Wegner[3],Michael W. Sereda[1,2,8] and Klaus-Armin Nave[1,8]

1: Max Planck Institute of Experimental Medicine, Department of Neurogenetics, Göttingen, Germany
2: University of Göttingen (UMG), Department of Clinical Neurophysiology, Göttingen, Germany
3: Institut für Biochemie, Emil-Fischer-Zentrum, Friedrich-Alexander Universität Erlangen-Nürnberg, Erlangen, Germany
4: Charité Universitätsmedizin Berlin, Neurocure Excellence Cluster, Institute of Cell and Neurobiology, Berlin, Germany
5: Laboratory of Molecular Biology (Celgen), Department of Development and Regeneration, University of Leuven, Leuven, Belgium
6: Centre for Neuroregeneration, University of Edinburgh, Edinburgh, United Kingdom
7: Institute of Molecular Health Sciences, Department of Biology, ETH Zürich, Zürich, Switzerland
8: These two authors jointly directed the study.
*: equal contribution

Correspondence:

Michael W. Sereda, M.D.
Department of Neurogenetics
Research Group Translational and Molecular Neurology
Max Planck Institute of Experimental Medicine
Hermann-Rein-Straße 3
37075 Göttingen
Phone: (0049) (0)551 3899 764
sereda@em.mpg.de

Klaus-Armin Nave, Ph.D.
Department of Neurogenetics
Max Planck Institute of Experimental Medicine
Hermann-Rein-Straße 3
37075 Göttingen
Phone: (0049) (0)551 3899 757
nave@em.mpg.de

Running title: ***Sip1* in Schwann cells**

Abstract

Schwann cell development and peripheral nerve myelination require the serial expression of transcriptional activators, such as Sox10, Oct6/Scip/Pou3f1 and Egr2/Krox20. Here we show that transcriptional repression, mediated by the zinc-finger protein Sip1, is essential for differentiation and myelination. Mice lacking *Sip1,* which is transiently expressed early in the Schwann cell lineage, develop a severe peripheral neuropathy, caused by the failure of axonal sorting and the virtual absence of myelin. Sip1-deficient Schwann cells continuously express repressors of lineage progression. Moreover, negative regulators of transcription, such as *Sox2 and Hey2*, emerge as direct Sip1 target genes, supporting a model of 'inhibition of inhibitors' in myelination control. When *Sip1* is deleted in adult mice, Schwann cells readily dedifferentiate following peripheral nerve injury and become 'repair cells'. However, nerve regeneration and remyelination are both impaired, demonstrating that Sip1, although undetectable in adult Schwann cells, has a latent function throughout life.

Introduction

The successive developmental stages of Schwann cell proliferation, axon sorting and myelination are regulated by a feed-forward cascade of transcriptional activators that ultimately up-regulate a large number of genes encoding myelination-associated enzymes and myelin structural proteins [1-3]. Well studied examples include the transcription factor *Krox20 (Egr2)*, as illustrated by *Krox20* mutant Schwann cells, which successfully sort axons but fail to generate or maintain myelin membranes [4]; [5]. Also the transcription factors *Oct6* and *Sox10*, developmentally upstream and directly interacting with *Krox20* promote Schwann cell differentiation and myelination [6,7]. *Sox10* null mutant mice die prenatally with a lack of peripheral glia, revealing an early function of this transcription factor in the neural crest lineage, whereas later Schwann cell-specific *Sox10* inactivation leads to developmental arrest at an immature stage [8,9].

Several transcription factors have also been identified as "negative regulators" of myelination, including both transcriptional activators (e.g. *Sox2*, *c-jun*, *Pax3, Notch-ICD)* and inhibitors (*Id2*). While the most likely function of these factors is driving Schwann cell "de-differentiation" after injury and in preparation for nerve repair (Jessen and Mirsky, 2008), their presence interferes with myelination and myelin maintenance. This raises the question how inhibitory regulators themselves are controlled during Schwann cell differentiation. Transcriptional repressors are plausible candidates. For example, the co-repressor Nab (NGFI-A/Egr-binding) is essential for PNS myelination [10]. However, when associated with Krox20 this protein is a co-activator of myelin protein genes, and the significance of gene repression by Nab/Krox20 complexes in Schwann cells is unclear [11,12]. Also the zinc-finger protein Ying-Yang (YY1), an essential transcriptional inhibitor in myelinating

oligodendrocytes (He et al., 2007), acts as a transcriptional activator in the peripheral nervous system (PNS), immediately upstream of Krox20 (He et al., 2010).

Smad-interacting protein-1 (Sip1, also known as Zeb2 or Zfhx1b) is a widely expressed zinc-finger homeobox protein, originally identified by its binding to Smad1 [13,14]. During epithelial to mesenchymal transition, SIP1 represses the transcription of several genes for cell adhesion molecules, such as E-cadherin [15-17]. In the central nervous system, newly born neurons express Sip1 to down-regulate signalling proteins that drive adjacent neurogenesis (Seuntjens et al., 2009). *Sip1* also regulates oligodendrocyte differentiation, because mutant cells fail to fully mature and make myelin [18].

Similar to the expression of *Sox10* in the PNS, Sip1 is also detectable early in the neural crest lineage [19]. In humans, mutations of *SOX10* and *SIP1* have been associated with the clinically related Waardenburg syndrome type 4 and Mowat-Wilson syndrome, respectively [20]. For neural crest cells, even direct interactions of SOX10 and SIP1 proteins have been proposed, but this is also difficult to reconcile with their respective roles as transcriptional activators and repressors [21]. Sip1 is a canonical transcriptional repressor and in crest-derived immature Schwann cells a candidate to 'release the brake' on differentiation that might be imposed by the negative regulators, such as Sox2.

Here, we show that Sip1 targets indeed inhibitors of Schwann cell differentiation. Mice lacking *Sip1* specifically in this lineage show a complete arrest of Schwann cell maturation and exhibit a virtually amyelinated phenotype. However, Sip1-deficient Schwann cells survive *in vivo* and maintain axonal integrity. While *Sip1* is not

required for adult myelin maintenance and axonal integrity, after injury *Sip1*-deficient Schwann cells fail to efficiently support nerve regeneration.

Results

SIP1 is expressed at early stages of Schwann cell development and after acute nerve injury

To explore SIP1 expression by Schwann cells, we immunostained paraffin sections of mouse sciatic nerves at different developmental stages. SIP1 was exclusively localized to cell nuclei. At E18.5, about 70% of Schwann cells were Sip1-positive. At age P10, only single cells could be immunostained, and at P25 virtually all Schwann cells were SIP1-negative (**Fig. 1a**).

To study the Schwann cell-specific function of Sip1, we bred *Sip1* floxed mice [22] to mice expressing Cre under control of the *desert hedgehog* promoter, leading to recombination in the Schwann cell lineage between embryonic days (E) 11 and 13.5 [9,23], when most cells are at the precursor stage [24]. Loss of Sip1 protein was confirmed by the absence of immunostaining (**Fig. 1a**).

To determine possible Sip1 re-expression in de-differentiating Schwan cells after acute sciatic nerve injury, we also stained paraffin sections of the distal segment at different time points after a nerve crush (**Fig. 1b**). Six hours after injury, about ten percent of Schwann cells were Sip1-positive (9.8±1.9%). A similar fraction could be stained after 24 hours (6.9±4.8%), but this number increased with a significant scatter between animals up to 50% (33.7±20.2%) after 3 days (**Fig. 1b**). However, on day 14 after crush, a time point when remyelination is at its peak, only a few percent of all Schwann cells still expressed SIP1 (3.5±1,4%). We never detected Sip1-positive cells in the contralateral unharmed nerve (**Fig. 1b**) at any of the time points

analysed. We conclude that SIP1 expression is transient in peripheral nerves, preceding myelination in development and remyelination after acute nerve injury.

Mice lacking Sip1 in Schwann cells display severe defects of axon sorting and myelination

Conditional mutants (*Dhh-Cre::Sip1*$^{flox/flox}$) were born at the expected Mendelian ratio and phenotypically distinguishable from littermate controls in the second postnatal week, when they had reduced body size and developed ataxia and hind limb weakness (**Suppl. Video 1**). The latter progressed with age but never led to complete hind limb paralysis. Surprisingly, when electrically stimulating the sciatic nerve of conditional mutants it was difficult to record any compound muscle action potential, unlike in controls, which suggests major conduction blocks (**Fig. 1f**). However, *Sip1* conditional mutants had a normal life span, and we only occasionally observed unexplained premature deaths.

To assess the developmental stage of Sip1-deficient Schwann cells in amyelinated nerves, we immunostained cross-sections from mutants and controls for Krox20 (also known as Egr2) and Sox2, as prototype positive and negative regulators, respectively. S100β was taken as a marker for both, immature and mature Schwann cells. While Schwann cells in control mice robustly expressed Krox20 and S100β and were negative for Sox2, only a few Sip1-deficient Schwann cells expressed Krox20 and S100β but about 30 percent were positive for Sox2 (**Fig.1 c-e**).

At P25, the sciatic nerves of mutant mice were thinner and more translucent than those of controls (**Fig. 2a,b**). Immunostaining of cross-sections for axonal β–tubulin (TuJ1) and myelin basic protein (MBP) revealed closely packed, amyelinated axons

in mutants but not in controls (**Fig. 2c,d**). Also by electron microscopy, *Sip1*-deficient mice lacked peripheral myelination and revealed abnormal axon bundles, with Schwann cells engulfing larger groups of axons that also greatly varied in diameter (**Fig.2 e,f,g,h,i**). Within these bundles, interdigitating Schwann cell processes could be observed, but the majority of axons remained closely packed, resembling axons associated with immature Schwann cells in embryonic nerves (**Fig. 2i**). Most Schwann cells even failed to establish the one-to-one relationship with axons. Here, we noticed that the basal lamina of *Sip1*-deficient Schwann cells was often thin, discontinuous, and not attached to the glial cell membrane, providing a plausible cause of failed axonal sorting ([25]). Many Schwann cells displayed also 'redundant basal lamina loops' (**Fig. 2g**).

At one year of age, peripheral axons had grown in diameter, but the overall pathology appeared unchanged (**Fig. 2j-m**). Compared to P25, the total Schwann cell number was unaltered in mutants and the percentage of BrdU-positive (proliferating) cells did not differ between mutants and controls, quantified at E18.5, P10 and P25 (**Suppl.Fig.1**). This suggests, that *Sip1*-deficient Schwann cells exit the cell cycle normally and survive in the absence of myelination.

At all time points studied (including 1 year of age) we found no evidence for axonal degeneration, except for rare axonal swellings (not shown). This suggests that *Sip1*-deficient Schwann cells can support axon survival, at least under conditions of reduced electrical activity and energy consumption, which is strongly suggested by the finding of conduction blocks (see above).

***Sip1*-deficient Schwann cells continuously express negative regulators of differentiation**

To further define the stage at which *Sip1*-deficient Schwann cells arrest in development, we performed a transcriptome analysis of sciatic nerves at age P25. Steady-state levels of more than 700 mRNAs differed (at least 2 fold) in abundance between the two genotypes. The 20 top up- and down-regulated genes are shown in **Fig. 3a**. We confirmed a subset of differentially regulated genes by quantitative real-time PCR, selecting promyelinating factors as well as negative regulators of myelination (note the logarithmic scale in **Fig. 3b,c**). As predicted from the phenotype of *Sip1*-conditional mutants and the histological analysis, genes encoding myelin proteins were down-regulated in mutants compared to controls (**Fig. 3c**). This was also the case for promyelinating factors of PNS myelination, such as *Oct6/SCIP* and *Krox20/Egr2* (**Fig. 3c**). Importantly, *Sip1*-deficient Schwann cells revealed the persistent expression of transcripts that are normally down-regulated at this age, (**Fig. 3b**). This includes the negative regulators of Schwann cell differentiation *(e.g. Sox2, c-jun*, *Id2*) and markers defining immature Schwann cells (e.g. *Brn2, Gfap*). Sip1-deficient Schwann cells also expressed very low amounts of *S100β*, a well-known marker of both immature and mature Schwann cells (**Fig. 3c**). In addition, we identified the *Notch* effector *Hey2* as one of the most strongly (16.7±1.4-fold) upregulated genes in our data set (**Fig. 3a,b**), as confirmed by quantitative PCR. Also other components of the *Notch* signaling cascade were upregulated in our microarray analysis in mutants compared to controls, such as *Notch1* (1.3-fold), *Hes1* (1.6-fold) and *jagged1* (1.9-fold), arguing for persistently activated, inhibitory Notch signaling in Sip1-deficient Schwann cells. Confirmed by RT-PCR, we also found highly elevated (13.4±3.1-fold) expression of the endothelin receptor B (*Ednrb*) gene, encoding an efficient repressor of Schwann cell differentiation upon ligand binding [26].

Taken together, *Sip1*-deficient Schwann cells are arrested at an early developmental stage, with a very low expression of maturation factors and persistent (abnormal) expression of several negative regulators.

Schwann cell Sip1 directly represses negative regulators of differentiation

To test for a possible direct effect of Sip1 as a repressor of relevant target genes, we performed luciferase gene reporter assays using the S16 Schwann cell line. Promoter regions of murine *Sox2*, *Hey2* and *Ednrb,* each containing putative Sip1 binding sites (CACCT, schematically depicted in **Fig. 3e**), were cloned into the pGL2-luciferase plasmid (Fig. 3d, e). Next, S16 cells were co-transfected with the resulting pGL2 fusion constructs and increasing amounts of a Sip1 expression plasmid in which the expression of Sip1 was under control of the CMV5 promoter (pCMV5-Sip1). In the analysis of the following luciferase assays, activity of lysates from S16 cells co-transfected with the pGL2-luc plasmid containing the respective promoter fragment and the empty pCMV5 plasmid was considered 100%. Co-transfection with the Sip1 expression construct led to a significant dose-dependent downregulation of luciferase activity when compared to co-transfection with the empty pCMV5 plasmid (**Fig. 3d**). This strongly suggests that the genes selected for proof-of-principle experiments are indeed direct targets of Sip1-mediated repression.

Sip1-mediated repression of *Ednrb* and *Hey2* is functionally relevant in Schwann cells *in vivo*.

To determine whether Sip1-mediated 'inhibition of inhibitors' is also functionally relevant *in vivo,* we generated *Sip1* double mutant mice, i.e. in combination with one of two negative regulators (Ednrb and Hey2) for which floxed mutants were available [27,28]. By crossbreeding, we obtained two genotypes (*Dhh-Cre::Sip1*$^{flox/flox}$*::Ednrb*$^{flox/flox}$

and *Dhh-Cre::Sip1*$^{flox/flox}$*::Hey2*$^{flox/flox}$), termed *Sip1/Ednrb-KO* and *Sip1/Hey2-KO* in the following. While we could not assume to reach a phenotypical "rescue" with the loss of only one inhibitor, we searched for histological signs of improvement in these double-mutants. We therefore immunostained cross-sections of sciatic nerves for Krox20 (**Fig. 1d**). Indeed, the number of labelled Schwann cell nuclei (in *Sip1*$^{fl/fl}$ controls 36.7±2.9 per section) was strongly reduced in *Sip1* single mutants (to 6.0±0.4), but increased significantly both in *Sip1/Ednrb-dcKO* (to 19.9±4.3) and in *Sip1/Hey2-dcKO* (to 16.8±2.9) sciatic nerves (**Fig. 4a,b).**

Also at the morphological level, axon-Schwann cell units appeared more matured in *Sip1/Ednrb* and in *Sip1/Hey2* conditional double-mutants, at least when compared to the large and unsorted fiber bundles of *Sip1* single mutants (**Fig. 4c**). Quantifying Remak-like (partially sorted) bundles with only 1-5 axons at age P25 (**Fig. 4d**), their number was higher in sciatic nerve cross sections of double mutants (*Sip1/Ednrb:* 51.1±9.4; *Sip1/Hey2*: 58.4±8.7) than *Sip1* single mutants (DhhCre::Sip1$^{fl/fl}$: 27.5±6.1). Thus, already the lack of one negative regulator (downstream of Sip1) improves the ability of *Sip1* mutant Schwann cells to initiate axon sorting.

Sip1-deficient Schwann cells are unable to efficiently support nerve regeneration

Since Schwann cells reexpressed Sip1 after an acute nerve injury (**Fig.1c**), we asked whether the induction of Schwann cell de-differentiation and peripheral nerve regeneration would be affected by the absence of Sip1. To this end we inactivated *Sip1* in Schwann cells of adult mice, using a tamoxifen-inducible PLPCreERT2 driver line [29]. Recombination was induced at 6-8 weeks of age and efficient CreERT2

expression was confirmed, using a reporter mouse that expresses tdTomato [30], on sciatic nerve cryostat sections (**Suppl.Fig.2**).

When *Plp-CreERT2::Sip1*$^{fl/fl}$ mice were analysed 12 weeks after the last tamoxifen injection, sciatic nerve morphology and myelin sheath thickness appeared unaltered (**Suppl. Fig.3**). We then performed sciatic nerve crushes in mice 4 weeks after the last tamoxifen (or vehicle) injection. Footprints on a walking track were used to monitor functional recovery. For histological analyses, animals were sacrificed 28 and 56 days after sciatic nerve crush. In these experiments, mice from the three control groups functionally recovered as expected and as measured by the sciatic functional index (SFI). However, *Plp-CreERT2::Sip1*$^{fl/fl}$ mice remained severely impaired until the end of this study (56 days after crush, **Fig. 5a**).

In physiological tests, carried out 52 days after sciatic nerve crush, *Sip1*-floxed control mice regained significant motor nerve conduction. We recorded a velocity (NCV) of about 18±2.9 m/s, which is about 70% of the NCV of an unharmed contralateral nerve (33±5.2 m/s), as determined in mice of either genotype.
In contrast, *Sip1* conditional mutants maintained severe axonal conduction problems that did not allow us to measure a NCV (**Fig. 5b,c**). Distal amplitudes (normal contralateral nerve: 29.8±10.1mV) were still reduced 52 days after crush injury in control mice (10.9±4.4 mV), but not even detectable in *Plp-CreERT2::Sip1*$^{fl/fl}$ mutants, indicating a regeneration failure with irreversible conduction blocks.

Indeed, when we immunostained sciatic nerve cross sections for myelin (MBP) and axons (Tuj1), virtually all fibers showed remyelination in control mice (**Fig.6a, top panel**), whereas in nerves of tamoxifen-induced *Plp-CreERT2::Sip1*$^{fl/fl}$ mutants we

observed large amyelinated fibers 8 weeks after injury (**Fig.6a, bottom panel**). We also analysed remyelination by electron microscopy (**Fig. 6b**). At 28 days and 56 days after crush injury mutants exhibited significantly fewer remyelinated axons (**Fig. 6c, upper panel**).

Interestingly, by g-ratio analysis axons remyelinated in mutant (*Plp-CreERT2::Sip1*$^{fl/fl}$) mice had the same myelin sheath thickness we determined in controls (**Suppl.Fig.4**). Also 56 days after crush, we still observed remyelinating Schwann cells with fewer, non-compacted myelin loops (**Fig. 6d**). Thus, given the timing of Sip1 re-expression after acute nerve trauma (**Fig.1c**), *Sip1* is likely required for early regenerative events, such Schwann cell "de-differentiation" or myelin repair.

***Sip1*-deficient Schwann cells do not fully redifferentiate after nerve injury**

To distinguish between alternative Sip1 functions after nerve injury, we studied sciatic nerves in tamoxifen-treated *Plp-CreERT2::Sip1*$^{fl/fl}$ mice 3 days after transection. At this time, there was no significant difference in the number of preserved myelin sheaths (1650±89 per section), when compared with vehicle-treated controls (1785±287) 2.0mm distal to the transection site (**Fig. 7a**).

Also steady-state mRNA levels of Schwann cell dedifferentiation markers (Jessen and Mirsky, 2008), such as *c-jun*, *Sox2* and *p75ntfR* were expressed at comparable levels in the distal stump (**Fig. 7b** and data not shown), whereas myelination markers, such as *Krox20* and *Mpz,* were downregulated in both, mutants and controls, when compared to the contralateral nerve (**Fig. 6b**). Taken together, the early steps of Schwann cell dedifferentiation are not perturbed by the lack of Sip1.

We next analysed at a functional level the regenerative axon outgrowth of crushed sciatic nerves in conditional Sip1 mutants and controls, using the "pinch test". When tested 4 days after injury, deeply anaesthetized mice of all three control groups showed a clear muscle reaction to a pinch of the sciatic nerve applied with a pair of forceps distal to the original crush site (**Fig. 7c**). However, the distance at which a response could be elicited differed between genotypes, with all control groups showing more efficient axon outgrowth (e.g. 6.6±0.8 mm in mice lacking Cre) compared to tamoxifen-treated *Sip1* mutants (5.4±1.3 mm).

We hypothesized, that reduced regenerative capacity is caused by poor Schwann cell differentiation. We therefore analysed the distal stump of sciatic nerves at a late time point (56 days after crush), when control mice had fully recovered (**Fig. 7d**). Indeed, in *Sip1* mutants we could still detect a significant expression of dedifferentiation markers, such as *Sox2* and *Id2* (**Fig. 7d**). Interestingly, *Hey2* mRNA was only upregulated in mutant nerves, an "ectopic" expression similar to that found in *Sip1*-deficient Schwann cells at age P25. In contrast, *Krox20* was downregulated in comparison to its expression in uninjured mutant nerves (**Fig.7d**). Taken together, *Sip1*-deficient Schwann cells can dedifferentiate after injury, but often fail to redifferentiate and provide myelin repair.

Discussion

We have identified an essential regulator of Schwann cell differentiation and peripheral myelination, the two-handed zinc finger/homeodomain protein Sip1. In contrast to previously described promyelinating transcription factors in the Schwann cell lineage, such as Oct6, Krox20, or Sox10, which activate the transcription of down-stream factors and ultimately myelin-associated genes, Sip1 is a transcriptional repressor and more widely expressed (Verschueren et al., 1999).

The developmental defect of conditional *Sip1* mutant mice is also more severe than that of *Oct6* or *Krox20* mutants. Deletion of *Oct6* causes only a transient arrest of Schwann cell differentiation after radial sorting, i.e. at the pro-myelin stage (Bermingham et al., 1996; Jaegle et al., 1996). Likewise, Schwann cells lacking *Krox20* are able to sort axons but then completely fail to myelinate (Topilko et al., 1994). Null mutant mice of *Sox10*, a gene already expressed in the emerging neural crest, die embryonically with a lack of all peripheral glia (Britsch et al., 2001). Only later cell-specific deletion of *Sox10* after Schwann cell specification (induced by *Dhh-Cre* as in *Sip1* cKO) leads to a similar developmental arrest in peripheral nerves with the lack of radial axonal sorting and a virtual absence of myelin (Finzsch et al., 2010). Early arrest of Schwann cell maturation has also been observed in the context of chromatin remodelling. Mice in which Schwann cells lack Brg1, a subunit of the BAF chromatin-remodelling complex that is recruited by Sox10, develop a severe peripheral neuropathy and die prematurely (Weider et al., 2012). In comparison, *Sip1* conditional mutants survive much better, despite the same sorting defect and lack of myelination. We speculate that Schwann cell-mediated axonal support, which

protects from conduction blocks and lethal breathing defects is largely independent of *Sip1*.

The hierarchical relationship of the known transcription factors in the Schwann cell lineage is complex, owing in part to their broad temporal expression domains and changing molecular interactions, including positive feedback loops (Stolt and Wegner, 2015). For example, *Krox20* is activated in Schwann cell precursors by the positive regulators Oct6 and Sox10, which then collectively upregulate genes for myelin proteins and enzymes of the lipid biosynthesis pathway. How are these feed-forward loops developmentally controlled? Our data on Sip1 suggest the existence of several brakes in the system, with the loss of Sip1 leading to continous expression of developmental inhibitors that block axonal sorting and myelination. This group of negative regulators is overlapping but not identical to other factors known to drive programmed de-differentiation of mature Schwann cells, such as c-Jun, after nerve injury (see below).

Whereas the morphological defects of dysmyelination are strikingly similar in conditional *Dhh-Cre*::*Sox10* and *Dhh-Cre*::*Sip1* mutant mice, it is surprising that in *Sip1*-deficient mice all Schwann cells survive. Despite the virtual absence of myelin and similarly severe neuropathy, conditional *Sip1* mutant mice have a normal life span, and Sip1-deficient Schwann cells support axon survival at least to some extent. We also note that in *Sip1*-deficient Schwann cells *Sox10* mRNA itself is unaltered in abundance (data not shown). The transcriptional (co-)activator Sox10 is expressed throughout the Schwann cell lineage and directly binds to Oct6 and Krox20, potentially affecting a broader set of myelin-associated genes (Ghislain and Charnay,

2006), including most likely those that are required for survival and axonal metabolic support.

By expression profiling of peripheral nerves from *Sip1* mutant mice and by functional analysis of different promoter-reporter constructs we have identified several direct target genes of Sip1, which include known negative regulators of myelination and factors previously associated with Schwann cell de-differentiation. Thus, our findings suggests that negative regulatory proteins such as Sox2, Hey2, or Ednbr1 need to be down-regulated early in development in order for Schwann cell differentiation, axonal sorting and myelination to proceed **(Fig. 8)**.

We cannot formally exclude that also transcriptional activation of unknown target genes by Sip1 (e.g. in combination with unknown coactivators) promotes Schwann cell differentiation in wild-type mice. However, the most likely explanation why conditional *Sip1* mutants display very low expression of Krox20 and other myelin protein genes is a secondary developmental arrest.

Since Sip1 itself is only transiently expressed, the down-regulation of its target genes ("inhibiting the inhibitors") most likely allows immature Schwann cells to overcome a developmental block, after which their further differentiation becomes Sip1-independent. At least two genes appear to contribute to this block (*Hey2* and *Ednbr2*) when studied along with *Sip1* in corresponding double-mutant mice, whose developmental potential is significantly improved, as quantified by the number of *Krox20* expressing Schwann cells. On the other hand, normally myelinated (adult wild-type) nerves, exhibit the absence of both Sip1 and its repressed target gene product(s), strongly suggesting that also factors other than Sip1 maintain the brake

on the expression of inhibitors and factors that would otherwise trigger de-differentiation. The identity of these repressors is not known. Epigenetic silencing, which has been studied at early stages of CNS myelination (Hernandez and Casaccia, 2015) could also play a role.

In our study, we identified Sip1 as a transcriptional repressor of *Ednrb* and *Sox2*, two known inhibitors of Schwann cell maturation, as well as of *Hey2*, a downstream effector of Notch signalling. We have selected these genes from a much larger group of abnormally up-regulated genes in order to show proof-of-principle for direct transcriptional repression by Sip1, as well as for their putative inhibitory function in Schwann cell differentiation. The latter was indeed possible in conditional double-knockout mice.

Two of these genes had been previously associated with the Schwann cell lineage. The endothelin B receptor (Ednrb) localizes to the plasma membrane of Schwann cell precursors and, upon binding of endothelin, delays the generation of mature Schwann cells, both *in vitro* and *in vivo* Indeed, *Ednrb* null mutant Schwann cells differentiate earlier than normal (Brennan et al., 2000; Stewart et al., 2001).

Sox2 is also a member of the Sry-related HMG box familiy of transcription factors, but (unlike Sox10) widely expressed and well known for its role in generating pluripotency (Masui et al., 2007). Sox2 is down-regulated early in Schwann cell development, coinciding with *Krox20* expression (Le et al., 2005a; Parkinson et al., 2008). Recently, it has been shown that overexpression of *Sox2* (a transcriptional activator) leads to persistent proliferation of Schwann cells and inhibits myelination,

implicating *Sox2* as a negative regulator of Schwann cell maturation *in vivo* (D. Parkinson, personal communication).

Hey2 is a member of the hairy and enhancer-of-split related bHLH transcription factor family that recruits histone deacetylases to repress transcription. The gene is expressed in spinal nerves and boundary cap cells until about embryonic day E17, when Schwann cell precursors become immature Schwann cells (Leimeister et al., 1999; Coulpier et al., 2009). In our analysis, *Hey2* is expressed at low levels in adult nerves, and not activated during injury-induced Schwann cell de-differentiation (Fig 7d and data not shown). We therefore found *Hey2* amongst the numerically most up-regulated mRNAs in sciatic nerves of *DhhCre::Sip1*$^{fl/fl}$ mice at age P25. Moreover, *Hey2* was strongly expressed in adult mutants 8 weeks after nerve injury. In both cases, "ectopic induction" of *Hey2* was a special feature of *Sip1*-deficient Schwann cells. The physiological function of *Hey2* in the Schwann cell lineage remains unknown. Conditional *Dhh-Cre::Hey2*$^{flox/flox}$ single mutants that we created in the course of our "rescue" experiments were normally developed and myelinated (data not shown).

In promoter-reporter cotransfection assays with a luciferase readout, Sip1 repressed transcription of the *Ednrb*, *Sox2* and *Hey2* promoters in a Schwann cell line. This identified all three inhibitory genes also as direct Sip1 targets.

One cannot assume that the phenotype of *Sip1* mutant mice can be "rescued" by introducing a second mutation into one gene for a (de-repressed) inhibitor. It is thus surprising that the additional deletion of either *Ednrb* or *Hey2* was sufficient to markedly increase the number of Krox20-positive Schwann cells and morphological

signs of sorting (more bundles with only 1-5 axons) in corresponding double-mutant mice. Experiments to find out whether these effects can be strengthened by targeting yet other genes and combining them in triple and quadruple mutants are important but beyond the scope of this first report.

With the lack of radial sorting, conditional *Sip1* mutants resemble mutants that lack normal basal lamina, such as beta 1 integrin and dystroglycan (Berti et al., 2011) or laminin 2 and 8 mutants (Yang, 2005). The basal lamina as a signalling platform between Schwann cell and the extracellular matrix is crucial for myelination as the analysis of numerous mouse mutant has shown (Feltri et al., 2008; Colognato and Tzvetanova, 2011). In conditional *Sip1* mutants, the basal lamina is thin, diffuse and often discontinuous. DRG/Schwann cell cocultures from *Sip1*-deficient mice on either collagen or artificial basal lamina did not result in myelination (not shown), suggesting that the abnormal basal lamina is not by itself the cause of dysmyelination, but rather a secondary effect.

In the CNS, myelination by oligodendrocytes is controlled in many ways by negative regulators. Direct interactions with signaling molecules, such as bone morphogenetic protein (BMP), Notch ligand, or Wnt proteins, can inhibit gene expression (Emery, 2010). At the molecular level, chromatin remodelling and epigenetic silencing of transcriptional repressors also follows the principle "inhibiting the inhibitors" (Li et al., 2009) . In oligodendrocyte development, Sip1 is also expressed, activated by Olig1 and Olig2, and essential for CNS myelination, as illustrated in *Olig-Cre::Sip1*$^{flox/flox}$ mice (Weng et al., 2012). Surprisingly, in oligodendrocytes Sip1 serves a dual role as a transcriptional activator of the Smad7 gene and it is the lack of this protein, which contributes to CNS dysmyelination in conditional mutant mice (Weng et al., 2012). In

our analysis, Smad7 was not expressed or dysregulated in PNS development of *Sip1* mutant mice (data not shown). Thus, despite some phenotypical resemblence, Sip1 serves different functions in PNS and CNS glial development.

When we deleted *Sip1* in Schwann cells of adult mice we found a severe delay in the regeneration and functional recovery after sciatic nerve crush injury. Even after eight weeks remyelination was not complete. Such a dramatic failure of myelin repair has only been described in mice lacking the AP1 transcription factor c-Jun in Schwann cells (Arthur-Farraj et al., 2012). However, in c-Jun mutant mice, already the formation of repair cells is perturbed, which are properly generated in the conditional *Sip1* mutants. Thus, the inability of Sip1 mutant Schwann cells to redifferentiate and to remyelinate marks a distinct developmental defect.

Figure legends

Figure 1. SIP1 expression in Schwann cell development and after injury. (a) Immunohistochemistry on sciatic nerve cross sections of wild type mice showing SIP1 expression at different developmental stages (red arrow heads, inset highlights one single SIP1-positive Schwann cell nucleus). SIP1 protein was virtually absent from Schwann cells of DhhCre::Sip1$^{fl/fl}$ mice at age E18.5 (inset highlights one single SIP1-negative Schwann cell nucleus). (b) SIP1 reexpression by mature Schwann cells at different time points after nerve crush (hpc: hours post crush, dpc: days post crush, ctrl: contralateral unharmed nerve) in distal stumps of injured sciatic nerves. (in (a) and (b): SIP1 brown, haematoxylin/nuclei blue, scale 10 µm, representative pictures of n=3 animals per time point and genotype except for the 14dpc time point n=4 and the contralateral nerve n=7, bars represent mean values +/- SD). (c) Representative traces of electrophysiological measurements after sciatic nerve stimulation from DhhCre::Sip1$^{fl/wt}$ and DhhCre::Sip1$^{fl/fl}$ mice at age P25. (d) Quantification of SIP1-positive nuclei shown in (b). (e)-(g) Immunohistochemistry on sciatic nerves cross sections of DhhCre::Sip1$^{fl/fl}$ mice and controls detecting KROX20 S100β and SOX2 (representative pictures of n=3 animals per genotype, KROX20, S100β and SOX2 are depicted in red, class III beta-tubulin (TuJ1) in green and DAPI in blue, scale 5 µm).

Figure 2. Mice lacking Sip1 in Schwann cells develop a severe neuropathy. Nerves of DhhCre::Sip1$^{fl/fl}$ mice (b) appeared translucent compared to controls (a) and did not show any myelin basic protein at age P25 (MBP) staining ((d), control in (c), MBP green, axons are stained in red by a class III beta-tubulin (TuJ1) antibody, representative images of n=3 animals per genotype). Axons in control nerves had

been sorted and fully myelinated (e), while mutant nerves displayed large axon Schwann cell families and did not show any myelin (f). (g) Sip1-deficient Schwann cell engulfing two axons and displaying supernumerary loops of basal lamina (red arrow heads). (h) More than 50 axons surrounded by a single Schwann cell in the nerve of a conditional Sip1 mutant (Schwann cell cytoplasm false-coloured in green). (i) Axons belonging to one bundle varied in size as illustrated by false colours (small axons: yellow, medium sized axon: red, large axon: purple). (j-m) Dysmyelination and large axon-Schwann cell families persisted to the age of one year (P365) in nerves of conditional mutants ((j) control, (k) and (m) mutant). One bundle of axons from a nerve of a conditional mutant at age P365 is depicted in (m). (Schwann cell cytoplasm false coloured in green, all images shown in g-m are representative of at least 3 animals per genotype and time point. Scale bars in all images 5 µm.

Figure 3. Sip1-deficient Schwann cells continuously express maturation inhibitors. (a) Heat map of a microarray analysis depicting the 20 most up- and downregulated genes in sciatic nerves of 3 DhhCre::Sip1$^{fl/fl}$ mice (mut) compared to those of 3 control littermates (ctrl) at age P25 (red: high expression, blue: low expression). A subset of promyelinating factors and maturation inhibitors were confirmed by quantitative realtime PCR ((b): upregulated genes; (c): downregulated genes, n=6 animals per genotype, bars depict mean values +/- SD, note the logarithmic scale). (d) Luciferase assays showing Sip1-dose-dependent diminished luciferase activity of Hey2, Ednrb and Sox2 promoter constructs upon cotransfection with a Sip1 expression plasmid (bars represent mean values of 3 independent experiments +/- SEM, activity of lysates from S16 cells co-transfected with the pGL2-luc plasmid containing the respective promoter fragment and the empty pCMV5

plasmid was considered 100%). (e) Scheme depicting the promoter fragments with predicted SIP1 binding sites used in (d).

Figure 4. Sip1-mediated repression of Ednrb and Hey2 is functionally relevant in Schwann cells. (a) A subpopulation of Schwann cells in both Ednrb/Sip1 and Hey2/Sip1 conditional double mutants are KROX20-positive, while only few cells in Sip1 conditional mutants display a KROX20 signal (KROX20: red, class III beta-tubulin (TuJ1): green, DAPI: blue, representative images of n=5 animals per genotype, scale 5 µm). (b) Quantification of KROX20-positive nuclei (data are presented as mean values +/- SEM, n=5 animals per genotype, except $Sip1^{fl/fl}$ n=3 animals, $Sip1^{fl/fl}$ vs. DhhCre::$Sip1^{fl/fl}$ P=0.008, DhhCre::$Sip1^{fl/fl}$ vs. DhhCre::$Sip1^{fl/fl}$::$Ednrb^{fl/fl}$ P=0.03, DhhCre::$Sip1^{fl/fl}$ vs. DhhCre::$Sip1^{fl/fl}$::$Hey2^{fl/fl}$ P=0.019, $Sip1^{fl/fl}$ vs. DhhCre::$Sip1^{fl/fl}$::$Hey2^{fl/fl}$ P=0.004, $Sip1^{fl/fl}$ vs. DhhCre::$Sip1^{fl/fl}$::$Ednrb^{fl/fl}$ P=0.018, two-sided student's t-test of unpaired samples). (c) Improved radial sorting and smaller axon Schwann cell families in conditional double (DhhCre::$Sip1^{fl/fl}$::$Ednrb^{fl/fl}$ or DhhCre::$Sip1^{fl/fl}$::$Hey2^{fl/fl}$) compared to single (DhhCre::$Sip1^{fl/fl}$) mutants (representative images of 5 animals per genotype, scale 10 µm) at age P25. (d) Significantly higher number of axon-Schwann cell units with 1 to 5 axons per Schwann cell in both double mutant mice at age P25 compared to Sip1 single mutants (n=5 animals per genotype, at least 22 randomly chosen axon Schwann cell families per animal, mean values +/-SEM, DhhCre::$Sip1^{fl/fl}$ vs. DhhCre::$Sip1^{fl/fl}$::$Ednrb^{fl/fl}$ P=0.046, DhhCre::$Sip1^{fl/fl}$ vs. DhhCre::$Sip1^{fl/fl}$::$Hey2^{fl/fl}$ P=0.02, two-sided student's t-test of unpaired samples).

Figure 5. Sip1 is crucial for functional recovery after injury. (a) Functional recovery of tamoxifen-treated PLPCreERT2::$Sip1^{fl/fl}$ mice (Cre+ fl/fl tamoxifen) was

significantly slower as determined by the sciatic functional index (SFI) compared to 3 control groups. (n=10 animals per group and time point, mean values +/- SD are shown). (b)-(d) Electrophysiological recordings after sciatic nerve stimulation 52 days after crush revealed a conduction block in tamoxifen-treated PLPCreERT2::Sip1$^{fl/fl}$ mice while control nerves had regained roughly 70% of the nerve conduction velocity of the contralateral unharmed nerve ((b) representative traces, (c) quantification of nerve conduction velocity, (d) distal amplitude, bars represent mean values +/- SD, n=8 animals Sip1$^{fl/fl}$ tamoxifen-treated, n=5 animals PLPCreERT2::Sip1$^{fl/fl}$ tamoxifen-treated).

Figure 6. Remyelination by Sip1-deficient Schwann cells is impaired. (a) Immunohistochemistry for class III beta-tubulin (TuJ1, red) and MBP (green) on wax sections of sciatic nerves 56 days after crush showing large amyelinated fibers in tamoxifen-treated PLPCreERT2::Sip1$^{fl/fl}$ mice (Cre+ fl/fl tamox, representative images of 3 animals per group). (b) Ongoing remyelination in nerves of tamoxifen-treated PLPCreERT2::Sip1$^{fl/fl}$ mice 56 days after nerve crush evident by few non-compact myelin wraps as well as thin compact sheaths (scale 5 µm, boxed areas magnified in right panel). (c) Conditional mutants display fibrosis and large unmyelinated axons 56 days after crush (bottom right panel, red arrow heads, scale 5 µm). (d) Significantly fewer remyelinated fibers in nerves of tamoxifen-treated PLPCreERT2::Sip1$^{fl/fl}$ mice 28 and 56 days after nerve crush (dpc, upper panel, bars represent mean values +/- SD, Sip1$^{fl/fl}$ tamoxifen-treated n=3, PLPCreERT2::Sip1$^{fl/fl}$ tamoxifen-treated n=4, 28 days P=0.023, 56 days P=0.0078; lower panel, bars represent mean values +/- SD, Sip1$^{fl/fl}$ tamoxifen-treated n=3, PLPCreERT2::Sip1$^{fl/fl}$ tamoxifen-treated n=4, myelinated P=0.036, amyelinated P=0.027, two-tailed student's t-test of unpaired samples).

Figure 7. Impaired redifferentiation of Sip1-deficient Schwann cells. (a) and (b) Unaltered number of remaining myelin profiles in tamoxifen-treated PLPCreERT2:Sip1$^{fl/fl}$ mice (red arrow heads, right panel) compared to controls (red arrow heads, left panel) shown by silver impregnation of the distal sciatic nerve stump 3 days after transection (scale in (a) 10 µm, n=3 mice per group, bars in (b) represent mean values +/- SD, student's t-test for unpaired samples, P=0.50). (c) Comparable steady-state levels of mRNAs for c-jun and Sox2 in distal stumps of sciatic nerves of PLPCreERT2::Sip1$^{fl/fl}$ mice and controls 3 days after transection. Krox20 and Mpz mRNAs were similarily downregulated in both groups (n=3 mice per group, expression in the contralateral unharmed nerve was set to 1, bars represent mean values +/- SD). (d) Increased levels of Sox2, Id2 and Hey2 mRNAs in tamoxifen-treated PLPCreERT2::Sip1$^{fl/fl}$ mice 56 days after nerve crush compared to controls. Krox20 levels remained low in nerves of mutants (bars represent mean values +/- SD, n=6 mice Cre+ fl/fl tamoxifen, n=5 mice fl/fl tamoxifen, n=5 mice contralateral). (e) Delayed early axon regrowth in tamoxifen-treated PLPCreERT2::Sip1$^{fl/fl}$ mice compared to controls 4 days after nerve crush as assessed by the pinch test (bars depict mean values +/- SD, n=13 mice per group except for fl/fl tamoxifen n=16, fl/fl Cre+ tamoxifen versus fl/fl Cre+ vehicle P=0.006, fl/fl Cre+ tamoxifen versus fl/fl tamoxifen P=0.0011, fl/fl Cre+ tamoxifen versus fl/fl vehicle P=0.0027, student's t-test of unpaired samples).

Figure 8. Hypothetical working model of Sip1 function in Schwann cells (adapted from Jessen and Mirsky, 2005). The development of immature Schwann cells (imSC, immature basal lamina depicted in orange) to mature myelinating Schwann cells (myelSC, mature basal lamina yellow) is driven by positive

transcriptional regulators (green arrow). In parallel, suppressors of maturation (red arrow) need to be silenced. This is achieved by SIP1 acting as an “inhibitor of inhibition” thereby promoting differentiation. Sip1-inactivation in the Schwann cell lineage (Sip1-deficient SC, altered basal lamina light orange) leads to continous expression of differentiation inhibitors, such as Sox2, c-jun and Ednrb, and aberrant expression of the transcriptional repressor Hey2. At the same time, mRNA levels of Oct6, Krox20 and the genes coding for myelin proteins are low compared to mature myelinating Schwann cells. After injury, c-jun drives generation of an active repair cell, while Sip1 is crucial for the redifferentiation to a remyelination-competent Schwann cell.

Supplementary Figure 1. Sip1-deficient Schwann cells survive and exit the cell cycle normally. (a) Unaltered levels of Schwann cell proliferation as detected by incorporation of Bromo-desoxyuridine (BrdU) in DhhCre::Sip1$^{fl/fl}$ mice compared to controls at E18.5, P10 and P25. Values are expressed as the percentage of BrdU-positive cells of all DAPI-positive nuclei +/- SD. (b) The number of Schwann cell nuclei per cross section of sciatic nerve was unaltered between conditional single mutants (DhhCre::Sip1$^{fl/fl}$) and both double conditional strains (DhhCre::Sip1$^{fl/fl}$::Ednrb$^{fl/fl}$ and DhhCre::Sip1$^{fl/fl}$::Hey2$^{fl/fl}$) at age P25. Additionally, the Schwann cell number of DhhCre::Sip1$^{fl/fl}$ mice at age P365 was unaltered compared to P25 (n=3 animals per age and genotype, all bars depict mean values +/- SD).

Supplementary Figure 2. Confirmation of recombination 4 weeks after the last tamoxifen-injection. 4 weeks after the last injection, endogenous tdTomato fluorescence (red) was observed in sciatic nerve cross sections of tamoxifen-treated PLPCreERT2::Sip1$^{fl/fl}$ mice (top panel), but not in treated Sip1$^{fl/fl}$ mice (bottom panel,

myelin/fluoromyelin in green, scale 10 µm, representative images from n=3 mice per genoytpe).

Supplementary Figure 3. Inactivation of Sip1 in adult mice. Myelin sheath thickness was unaltered 12 weeks after the last injection in tamoxifen-treated PLPCreERT2::Sip1$^{fl/fl}$ mice compared to the 3 respective control groups. Representative images are shown in (a), a scatter plot depicting the gratio in relation to the fiber diameter for tamoxifen-treated PLPCreERT2::Sip1$^{fl/fl}$ mice compared to tamoxifen-terated Sip1$^{fl/fl}$ mice in (b), (n=3 animals per group, at least 100 randomly chosen fibers per animal, scale in (a) 5 µm).

Supplementary Figure 4. Unaltered myelin sheath thickness after remyelination. Scatter plot depicting the gratio in relation to the fiber diameter of remyelinated fibers 8 weeks after nerve crush. No significant difference in myelin sheath thickness was observed between tamoxifen-treated PLPCreERT2::Sip1$^{fl/fl}$ mice and the 3 respective control groups (n=3 animals per group, at least 100 randomly chosen fibers per animal).

Supplementary Video 1 DhhCre::Sip1$^{fl/fl}$ mouse walking on a grid showing atactic movements and hind limb weakness.

Materials and Methods

Mutant and transgenic mice

All experiments involving mice were conducted according to the Lower Saxony State regulations for the use of experimental animals in Germany as approved by the Niedersächsisches Landesamt für Verbraucherschutz und Lebensmittelsicherheit (LAVES) and performed in compliance with the animal policies of the Max Planck Institute of Experimental Medicine. Mice were housed in individually vented cages with a 12 hour light/dark cycle. Male and female mice were included in all experiments and randomly assigned to experimental groups according to age and genotype. $Sip1^{fl/fl}$ mice [22] were bred to DhhCre transgenic mice [23]. DhhCre::$Sip1^{fl/fl}$::$Ednrb^{fl/fl}$ mice were generated by breeding DhhCre::$Sip1^{fl/wt}$::$Ednrb^{fl/fl}$ mice to $Sip1^{fl/fl}$::$Ednrb^{fl/fl}$ mice [27]. Floxed Hey2 mice (Xin et al., 2007) were acquired from Jackson laboratories. DhhCre::$Sip1^{fl/fl}$::$Hey2^{fl/fl}$ mice were generated by breeding DhhCre::$Sip1^{fl/wt}$::$Hey2^{fl/fl}$ mice to $Sip1^{fl/fl}$::$Hey2^{fl/fl}$ mice. Floxed (double floxed) littermates were used as experimental controls in all experiments unless indicated otherwise. PLPCreERT2::$Sip1^{fl/fl}$ mice were generated by breeding $Sip1^{fl/fl}$ mice to PLPCreERT2 mice [29]. Sip1 floxed mice, *Hey2* floxed mice, PLPCreERT2 mice, and DhhCre mice were on C57/Black6 background, *Ednrb* floxed mice were on mixed C57Bl/6-SV129 background. Genotyping was performed on DNA isolated from tail or ear biopsies according to routine PCR methods using the following primers:
DhhCre sense 5'-CCTGCGGAGATGCCCAATTG-3' antisense 5'-CAGCCCGGAC CGACGATGAA-3' Sip1 floxed sense 5'-TGGACAGGAACTTGCATATGCT-3' anti-sense 5'-GTGGACTCTACATTCTAGATGC-3' Hey2 floxed sense 5'-CTAGAGAGG ACCTGGAGAGTTTAAG-3' antisense 5'-CTGTGCCACCAGCCTTAAAACC-3' Ednrb wild type allele sense 5'-CTGAGGAGAGCCTGATTGTGCCAC-3' antisense 5'-CGAC TCCAAGAAGCAACAGCTCG -3' Ednrb floxed allele sense 5'-TGGAATGTGTGCGA

GGCC -3' Ednrb floxed allele antisense 5'-CAGCCAGAACCACAGAGACCACCC -3' PLPCreERT2 transgene sense 5'-TGGACAGCTGGGACAAAGTAAGC -3' antisense 5'-CGTTGCATCGACCGGTAATGCAGGC -3'.

Statistics

Values are expressed as mean value +/- standard deviation (SD) unless indicated otherwise. Statistics were performed using the two-tailed Student's t-test for unpaired samples assuming unequal variance and P values below 0,05 were considered significant (* <0,05; ** <0,01; *** <0,001). Normal distribution of data was assumed, but not formally tested.

Induction of recombination, surgical procedures and foot print analysis

PLPCreERT2::Sip$^{fl/fl}$ mice and Sip1$^{flox/flox}$ mice were treated twice for 5 consecutive days with one daily intraperitoneal injection of 1 mg tamoxifen in corn oil with 10% analytical ethanol (all from Sigma) or the corn oil/ethanol mixture only (vehicle). Sciatic nerve crush or transection was performed under deep surgical anaesthesia (ketaminhydrochloride 100 mg/kg and xylazinhydrochloride 5 mg/kg) at the sciatic notch. For crush injuries, the nerve was compressed for 15 seconds with fine forceps. To test early axon outgrowth ("pinch test"), mice were deeply anaesthetized 4 days after crush injury, the sciatic nerve was completely exposed and pinched with fine forceps starting from the distal end until a muscle reaction was observed. The observer was blinded regarding genotype and treatment of the mice and the regeneration distance (distance from the crush site to the pinch site where a reaction was observed) was measured with a ruler in situ. Footprints were acquired during the light phase by painting the hind feet of mice with black colour and letting them run along a 50 cm walking track. Prints were digitalized and the distance between toe 1

and 5 and the length of the print measured using the FOOTPRINTS program [31]. The sciatic functional index was calculated according to [32]. The observer was blinded regarding the genotype of the mice.

Electrophysiological measurements

Electrophysiological measurements were performed under deep surgical anaesthesia (ketaminhydrochloride 100 mg/kg and xylazinhydrochloride 5 mg/kg). Two recording electrodes were inserted into the intrinsic foot muscle, distal stimulation electrodes were inserted at the ankle, and proximal stimulation electrodes were inserted at the sciatic notch. Compound muscle action potentials (CMAPs) were recorded with a Jaeger-Toennies Neuroscreen instrument. Nerve conduction velocities were calculated from the distance between proximal and distal stimulation electrodes (measured in situ) and the latency difference between the CMAPs after successive proximal and distal stimulation. CMAP amplitudes were calculated peak to peak.

Morphology, silver impregnation and electron microscopy

For ultrastructural analysis, nerves were immersion fixed in 2.5% glutardialdehyde and 4% paraformaldehyde in phosphate buffer and embedded into epoxy resin (Serva). Semithin sections were cut at a thickness of 0,5 µm (Leica RM 2155 using a diamond knife Histo HI 4317, Diatome) and stained with a mixture of 1% toluidine blue and 1% azur II or silver impregnated (Gallyas, 1979). Ultrathin sections were cut at a thickness of 50 nm, treated with uranyl acetate and lead citrate and analysed with a Zeiss EM 900 (Leo). The gratio was defined as the numerical ratio between the fiber diameter and the diameter of the same fiber including its myelin sheath and measured on electron micrographs for at least 100 randomly chosen axons per animal and nerve (3 animals per genotype and/or treatment group). Remyelinated

fibers after sciatic nerve crush were counted on complete semithin cross sections of sciatic nerves (n=3 animals per genotype and/or treatment group). The percentage of myelinated and unmyelinated axons 56 days after nerve crush was quantified by counting all fibers on 25 randomly taken electron micrographs at 3000x magnification per animal (n=3 animals per genotype and treatment group). Axons per bundle were quantified on electron microscopic images by analysing all axon Schwann cell units where the nucleus of the Schwann cell was visible (amounting to at least 22 randomly chosen axon-Schwann cell units per animal and nerve, 3 animals per genotype). For gratio analysis, quantification of remyelinated fibers and quantification of axons per Schwann cell, the observer was blinded regarding the genotype and/or treatment (tamoxifen or vehicle) of the animals.

Immunohistochemistry

Samples were immersion fixed using 4% phosphate buffered paraformaldehyde and embedded into paraffin wax. Immunohistochemistry was performed on 5 µm thick sections using the $LSAB_2$ system (DAKO) or secondary antibodies coupled to a fluorophore (Alexa555 or -488 donkey anti mouse, all from Molecular Probes diluted 1:2000). For heat-induced antigen retrieval, slides were boiled for 20 minutes in citrate buffer pH 6. The following primary antibodies were used: *Sip1* (SC27-1984, Santa Cruz: 1:200), betaIII-tubulin (MMS-435P, Covance 1:250), MBP (A0623, DAKO 1:500), Krox20 (rabbit, generous gift of Dies Meijer 1:500), Sox2 (SC1002, Millipore 1:200), S100β (AB52642, Abcam, 1:500). For each staining, samples from at least 3 individual animals per genotype (or treatment group) were processed simultaneously and used for the analysis. Sections were examined with a Zeiss Observer fluorescence microscope or Zeiss Axiophot brightfield microscope and

images acquired with Openlab 3.1.1 software (Improvision). Images were processed with Adobe Photoshop 12.0.4, Adobe Illustrator CS5 and NIH Image J 1.46R.

RNA preparation, cDNA synthesis, realtime PCR and microarray analysis

RNA was isolated from sciatic nerves using the RNeasy Kit (Qiagen) according to manufacturer's instructions and the concentration and quality (ratio of absorption at 260/280 nm) evaluated using the NanoDrop spectrophotometer. Reverse transcription was performed with 1 µg of total RNA using the Superscript Kit (Invitrogen) and random nonamer primers. Quantitative realtime PCR was performed in triplicate for each sample using SybrGreen (Life Technologies) and the ABI PRISM 7700 detection system (Perkin Elmer). Four mice per genotype and/or treatment group were used in each experiment unless specified otherwise, relative mRNA concentrations were determined using the threshold cycle method and normalized to Rpl8. Primer pairs: *Sox2* sense 5'-TCCAAAAACTAATCACAACAATCG-3' antisense 5'-GAAGTGCAATTGGGATGAAAA-3' Id2 sense 5'-GACAGAACCAGGCGTCCA-3' antisense 5'-AGCTC AGAAGGGAATTCAGATG-3' Oct6 sense 5'-AGCACTCGGACGAGGATG-3' antisense 5'-TTGAACTGCTTGGCGAACT-3' p75NTR sense 5'-CGGTGTGCGAGGACACT GAGC-3' antisense 5'-TGGGTGCTGGGTGTTGTGACG-3' c-jun sense 5'-CTGAGTG TGCGAGAGACAGC-3 antisense 5'-CCAAGTCCGTCCGTCTGT-3' *Krox20* sense 5'-AATGGCTTGGGACTGACTTG-3' antisense 5'-GCCAGAGAAACCTCCATTCA-3' MPZ sense 5'-ACTTGGCCTTCCCATCTCTC-3' MPZ antisense 5'-GGGCCACCAG AAGGTAGG-3' *Sip1* sense 5'-CAAGAGGCGCAAACAAGC-3' antisense 5'-TGCGTC CACTACGTTGTCAT-3' *Hey2* sense 5'-ATTGCAAATGACAGTGGATCAT-3' antisense 5'-AGCATGGGCATCAAAGTAGC-3' Rpl8 sense 5'-CAACAGCGCCGTTGTTGG T-3 antisense 5'-CAGCCTTTAAGATAGGCTTGTCA-3'.

P values for quantitative realtime PCR experiments are as follows: Figure 3b: Gfap 0.026, Hey2 P=4.57E-05, Ednrb P=0.002, Sox2 P=1.4E-05, Brn2 P=0.0006, Id2 P=0.0004, c-jun P=0.008, N-cad P=8.18E-06; figure 3c: Pmp2 P=3.5E-05, Mpz P=0.0001, Cnp1 P=9.56E-05, Krox20 P=0.002, Oct6 P=0.001, S100β P=0.002, p75Ntfr P=0.005, Erb3 P=0.0003, E-cad P=0.0006, Itga4 P=0.0003. Figure 7c: c-jun: fl/fl vehicle vs. fl/fl tamoxifen P=0.236, fl/fl vehicle vs. Cre+ fl/fl tamoxifen P=0.99, fl/fl vehicle vs. Cre+ fl/fl vehicle P=0.065, fl/fl tamoxifen vs. Cre+ fl/fl tamoxifen P=0.692; Cre+ fl/fl vehicle vs. Cre+ fl/fl tamoxifen P=0.263, Cre+ fl/fl vehicle vs. fl/fl tamoxifen P=0.14; Sox2: fl/fl vehicle vs. fl/fl tamoxifen P=0.144, fl/fl vehicle vs. Cre+ fl/fl tamoxifen P=0.53, fl/fl vehicle vs. Cre+ fl/fl vehicle P=0.476, fl/fl tamoxifen vs. Cre+ fl/fl tamoxifen P=0.386; Cre+ fl/fl vehicle vs. Cre+ fl/fl tamoxifen P=0.256, Cre+ fl/fl vehicle vs. fl/fl tamoxifen P=0.07; Krox20: fl/fl vehicle vs. fl/fl tamoxifen P=0.344, fl/fl vehicle vs. Cre+ fl/fl tamoxifen P=0.215, fl/fl vehicle vs. Cre+ fl/fl vehicle P=0.027, fl/fl tamoxifen vs. Cre+ fl/fl tamoxifen P=0.471; Cre+ fl/fl vehicle vs. Cre+ fl/fl tamoxifen P=0.083, Cre+ fl/fl vehicle vs. fl/fl tamoxifen P=0.067; Mpz: fl/fl vehicle vs. fl/fl tamoxifen P=0.449, fl/fl vehicle vs. Cre+ fl/fl tamoxifen P=0.391, fl/fl vehicle vs. Cre+ fl/fl vehicle P=0.216, fl/fl tamoxifen vs. Cre+ fl/fl tamoxifen P=0.184; Cre+ fl/fl vehicle vs. Cre+ fl/fl tamoxifen P=0.369, Cre+ fl/fl vehicle vs. fl/fl tamoxifen P=0.135; Figure 7d: Sox2: contralateral (ctrl) vs. fl/fl tamoxifen P=0.001, ctrl vs. Cre+ fl/fl tamoxifen P=0.001, fl/fl tamoxifen vs. Cre+ fl/fl tamoxifen P=0.007; Id2: ctrl vs. fl/fl tamoxifen P=0.0004, ctrl vs. Cre+ fl/fl tamoxifen P=3.003E-05, fl/fl tamoxifen vs. Cre+ fl/fl tamoxifen P=0.01; Hey2: ctrl vs. fl/fl tamoxifen P=0.0003, ctrl vs. Cre+ fl/fl tamoxifen P=0.0003, fl/fl tamoxifen vs. Cre+ fl/fl tamoxifen P=0.0001; Krox20 ctrl vs. fl/fl tamoxifen P=0.69, ctrl vs. Cre+ fl/fl tamoxifen P=0.0014, fl/fl tamoxifen vs. Cre+ fl/fl tamoxifen P=0.01).

Microarray analysis was performed at the Transcriptome Analysis Laboratory (TAL) of the University Göttingen using the Affymetrix GeneChip Mouse Gene 1.0 ST platform. 3 animals per genotype were compared and genes were considered to be regulated when changes were at least 2 fold up or down compared to controls.

Luciferase reporter assay

Promoter regions (mouse genome version mm10) for analysis of Sip1 binding were chosen using the eukaryotic promoter database (http://epd.vital-it.ch/). The Sox2 promoter region (chromosome 3 between positions 34,648,778 - 34,650,029) is localized relative to the transcriptional start site of the Sox2 gene -1239bp to +51bp. The Hey2 promoter region (chromosome 10 between positions 30,842,764 - 30,845,280) is localized relative to the transcriptional start site of the Hey2 gene -2499bp to +18bp. The Ednrb promoter region (chromosome 14 between positions 103,844,229 - 103,846,824) is localized relative to the transcriptional start site of the Ednrb gene (variant EdnRB_1) -2497bp to +99bp. Promoter regions were amplified by PCR and inserted as XhoI/XmaI fragments upstream of the luciferase gene into pGL2-luc (Promega). The following primers were used for the amplification of promoter regions: for Sox2 5´GCGCcccgggGGCAGGCAAGATTCTTGAAC 3´ and 5´ GCGCctcgagCTCTGCCTTGACAACTCCTG 3´, for Hey2 5´GCGCcccgggCTCTGAC CCAGACGTAGGAC 3´ and 5´ GCGCctcgagCGGCTCCTGGAGGTTCTTTC 3´ and for EdnRB 5´GCGCcccgggGGTAGTTTAATGCGCCCATC 3´ and 5´GCGCctcgagGC TGCTCCTAAACAGGCCTC 3´.

For luciferase reporter gene assays, the S16 Schwann cell line was used. Cells were transfected using polyethylenimin (PEI) on 3.5 cm tissue culture plates with 1.5 µg of luciferase reporter (pGL2-luc) and varying amounts (0.3 µg, 0.9 µg or 1.5 µg) of pCMV5-Sip1expression vector. Cells were generally harvested 48 h post-transfection

and luciferase activity was determined in the presence of luciferin substrate by detection of chemiluminescence. Single values: Ednrb 0.3 µg Sip1 plasmid 91% +/- 2.7, 0.9 µg 63% +/- 3.9, 1.5 µg 58% +/- 3.5, Sox2 0.3 µg Sip1 plasmid 85% +/- 5, 0.9 µg 41% +/- 6.8, 1.5 µg 26% +/- 2.3, Hey2 0.3 µg Sip1 plasmid 93% +/- 11.4, 0.9 µg 68% +/- 3.3, 1.5 µg 41% +/- 9.6).

Supplementary Methods

BrdU injections and immunohistochemistry

Bromodesoxiuridine (BrdU) was solubilized in water at a concentration of 10 mg/ml. Mice at the age of 10 or 25 days were injected intraperitoneally with one pulse of 100 µg/g body weight and sacrificed 4 hours later. Pregnant female mice at E18.5 were treated the same way and sacrificed 70 minutes after the pulse. Sciatic nerves were embedded into wax and cut at a thickness of 5 µm. For detection of BrdU-positive nuclei, sections were boiled for 5 minutes at 100W in a microwave in citrate buffer pH6, incubated for 30 minutes at room temperature in 0.2 M glycine followed by two washes in 100 mM disodium tetraborate pH 8.5. Anti-BrdU antibody (MAB3424, Millipore) was diluted 1:200 in 2% goat serum in PBS and applied over night at 4°C. After washing, the secondary antibody (Alexa555-anti-mouse, 1:2000, A-31570, Molecular Probes) and DAPI (0.05 µg/ml) were applied for 1 hour at room temperature. For quantification of proliferating cells, all BrdU/DAPI-positive nuclei were counted on cross sections of sciatic nerves and values expressed as percentage of BrdU-positive cells relative to all DAPI-positive nuclei.

References

1. Jessen, K. R. & Mirsky, R. Negative regulation of myelination: Relevance for development, injury, and demyelinating disease. *Glia* **56,** 1552–1565 (2008).
2. Monk, K. R., Feltri, M. L. & Taveggia, C. New insights on schwann cell development. *Glia* **63,** 1376–1393 (2015).
3. Stolt, C. C. & Wegner, M. Schwann cells and their transcriptional network: Evolution of key regulatorsof peripheral myelination. *Brain Research* 1–10 (2015). doi:10.1016/j.brainres.2015.09.025
4. Topilko, P. *et al.* Krox-20 controls myelination in the peripheral nervous system. *Nature* **371,** 796–799 (1994).
5. Decker, L. Peripheral Myelin Maintenance Is a Dynamic Process Requiring Constant Krox20 Expression. *Journal of Neuroscience* **26,** 9771–9779 (2006).
6. Ghislain, J. & Charnay, P. Control of myelination in Schwann cells: a Krox20 cis-regulatory element integrates Oct6, Brn2 and Sox10 activities. *EMBO Rep.* **7,** 52–58 (2006).
7. Kuhlbrodt, K., Herbarth, B., Sock, E., Hermans-Borgmeyer, I. & Wegner, M. Sox10, a novel transcriptional modulator in glial cells. *J. Neurosci.* **18,** 237–250 (1998).
8. Britsch, S. The transcription factor Sox10 is a key regulator of peripheral glial development. *Genes & Development* **15,** 66–78 (2001).
9. Finzsch, M. *et al.* Sox10 is required for Schwann cell identity and progression beyond the immature Schwann cell stage. *The Journal of Cell Biology* **189,** 701–712 (2010).
10. Le, N. *et al.* Nab proteins are essential for peripheral nervous system myelination. *Nature Neuroscience* **8,** 932–940 (2005).
11. Desmazieres, A., Decker, L., Vallat, J. M., Charnay, P. & Gilardi-Hebenstreit, P. Disruption of Krox20-Nab Interaction in the Mouse Leads to Peripheral Neuropathy with Biphasic Evolution. *Journal of Neuroscience* **28,** 5891–5900 (2008).
12. Mager, G. M. *et al.* Active Gene Repression by the Egr2{middle dot}NAB Complex during Peripheral Nerve Myelination. *Journal of Biological Chemistry* **283,** 18187–18197 (2008).
13. Verschueren, K. *et al.* SIP1, a Novel Zinc Finger/Homeodomain Repressor, Interacts with Smad Proteins and Binds to 5'-CACCT Sequences in Candidate Target Genes. *Journal of Biological Chemistry* **274,** 20489–20498 (1999).
14. Conidi, A. *et al.* Cytokine & Growth Factor Reviews. *Cytokine and Growth Factor Reviews* **22,** 287–300 (2011).
15. Comijn, J. *et al.* The two-handed E box binding zinc finger protein SIP1 downregulates E-cadherin and induces invasion. *Mol. Cell* **7,** 1267–1278 (2001).
16. Vandewalle, C. SIP1/ZEB2 induces EMT by repressing genes of different epithelial cell-cell junctions. *Nucleic Acids Research* **33,** 6566–6578 (2005).
17. Dai, Y.-H. *et al.* ZEB2 Promotes the Metastasis of Gastric Cancer and Modulates Epithelial Mesenchymal Transition of Gastric Cancer Cells. *Dig Dis Sci* **57,** 1253–1260 (2012).
18. Weng, Q. *et al.* Dual-Mode Modulation of Smad Signalingby Smad-Interacting Protein Sip1 Is Required for Myelination in the Central Nervous System. *Neuron* **73,** 713–728 (2012).
19. Van de Putte, T., Francis, A., Nelles, L., van Grunsven, L. A. & Huylebroeck, D. Neural crest-specific removal of Zfhx1b in mouse leads to a wide range of

neurocristopathies reminiscent of Mowat-Wilson syndrome. *Human Molecular Genetics* **16,** 1423–1436 (2007).
20. Mowat, D. R. *et al.* Hirschsprung disease, microcephaly, mental retardation, and characteristic facial features: delineation of a new syndrome and identification of a locus at chromosome 2q22-q23. *J. Med. Genet.* **35,** 617–623 (1998).
21. Stanchina, L., Van de Putte, T., Goossens, M., Huylebroeck, D. & Bondurand, N. Developmental Biology. *Developmental Biology* **341,** 416–428 (2010).
22. Higashi, Y. *et al.* Generation of the floxed allele of the SIP1 (Smad-interacting protein 1) gene for Cre-mediated conditional knockout in the mouse. *genesis* **32,** 82–84 (2002).
23. Jaegle, M. The POU proteins Brn-2 and Oct-6 share important functions in Schwann cell development. *Genes & Development* **17,** 1380–1391 (2003).
24. Jessen, K. R. & Mirsky, R. The origin and development of glial cells in peripheral nerves. *Nat Rev Neurosci* **6,** 671–682 (2005).
25. Colognato, H. & Tzvetanova, I. D. Glia unglued: How signals from the extracellular matrix regulate the development of myelinating glia. *Devel Neurobio* **71,** 924–955 (2011).
26. Brennan, A. *et al.* Endothelins control the timing of Schwann cell generation in vitro and in vivo. *Developmental Biology* **227,** 545–557 (2000).
27. Druckenbrod, N. R., Powers, P. A., Bartley, C. R., Walker, J. W. & Epstein, M. L. Targeting of endothelin receptor-B to the neural crest. *genesis* **46,** 396–400 (2008).
28. Xin, M. *et al.* Essential roles of the bHLH transcription factor Hrt2 in repression of atrial gene expression and maintenance of postnatal cardiac function. *Proc Natl Acad Sci USA* **104,** 7975–7980 (2007).
29. Leone, D. P. *et al.* Tamoxifen-inducible glia-specific Cre mice for somatic mutagenesis in oligodendrocytes and Schwann cells. *Molecular and Cellular Neuroscience* **22,** 430–440 (2003).
30. Madisen, L. *et al.* nn.2467. *Nature Neuroscience* **13,** 133–140 (2009).
31. Klapdor, K., Dulfer, B. G., Hammann, A. & Van der Staay, F. J. A low-cost method to analyse footprint patterns. *Journal of Neuroscience Methods* **75,** 49–54 (1997).
32. Inserra, M. M., Bloch, D. A. & Terris, D. J. Functional indices for sciatic, peroneal, and posterior tibial nerve lesions in the mouse. *Microsurgery* **18,** 119–124 (1998).

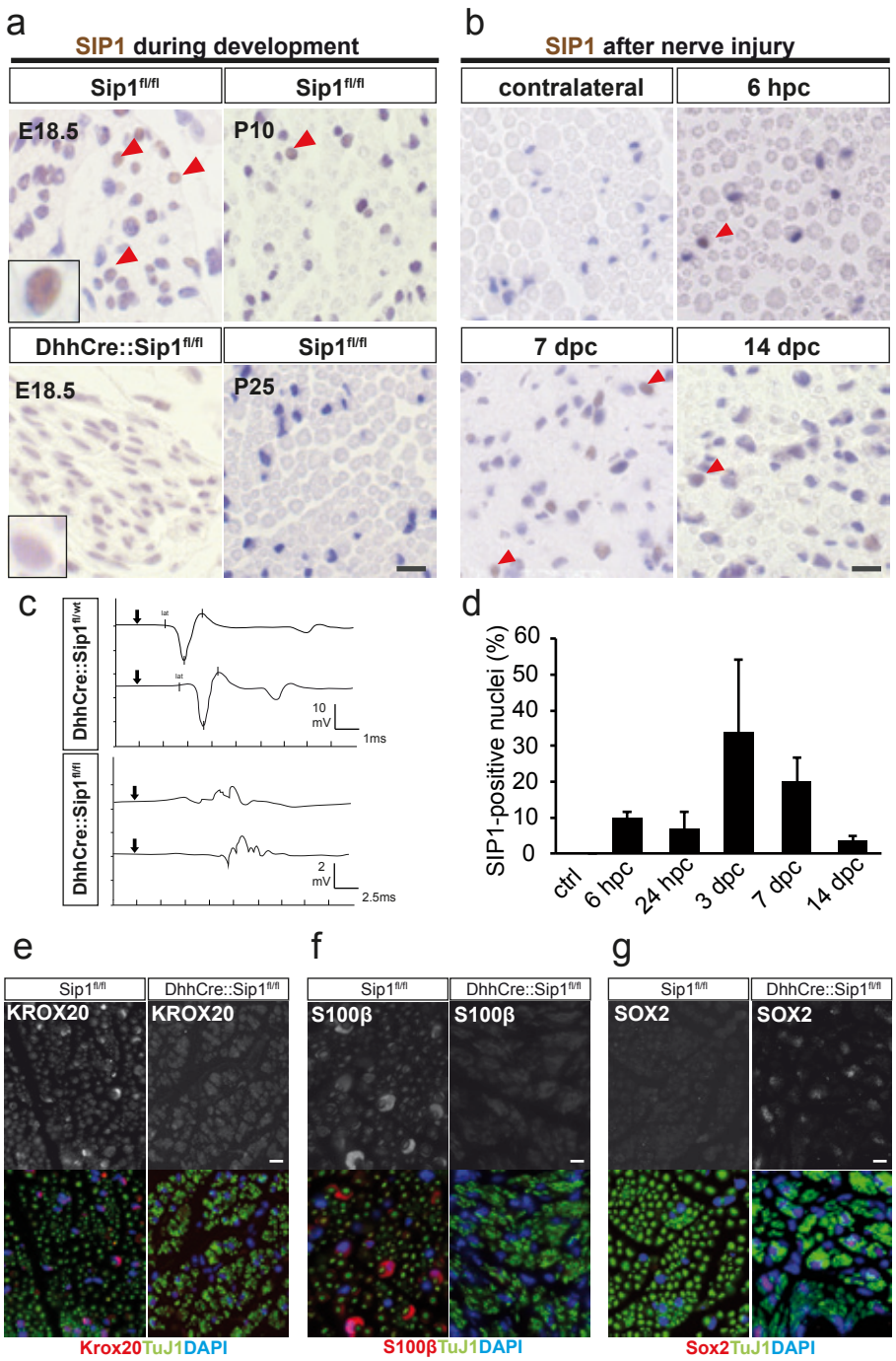

Figure 1. SIP1 expression in Schwann cell development and after injury. (a) Immunohistochemistry on sciatic nerve cross sections of wild type mice showing SIP1 expression at different developmental stages (red arrow heads, inset highlights one single SIP1-positive Schwann cell nucleus). SIP1 protein was virtually absent from Schwann cells of DhhCre::Sip1$^{fl/fl}$ mice at age E18.5 (inset highlights one single SIP1-negative Schwann cell nucleus). (b) SIP1 reexpression by mature Schwann cells at different time points after nerve crush (hpc: hours post crush, dpc: days post crush, ctrl: contralateral unharmed nerve) in distal stumps of injured sciatic nerves. (in (a) and (b): SIP1 brown, haematoxylin/nuclei blue, scale 10 µm, representative pictures of n=3 animals per time point and genotype except for the 14dpc time point n=4 and the contralateral nerve n=7, bars represent mean values +/- SD). (c) Representative traces of electrophysiological measurements after sciatic nerve stimulation from DhhCre::Sip1$^{fl/wt}$ and DhhCre::Sip1$^{fl/fl}$ mice at age P25. (d) Quantification of SIP1-positive nuclei shown in (b). (e)-(g) Immunohistochemistry on sciatic nerves cross sections of DhhCre::Sip1$^{fl/fl}$ mice and controls detecting KROX20 S100β and SOX2 (representative pictures of n=3 animals per genotype, KROX20, S100β and SOX2 are depicted in red, class III beta-tubulin (TuJ1) in green and DAPI in blue, scale 5 µm).

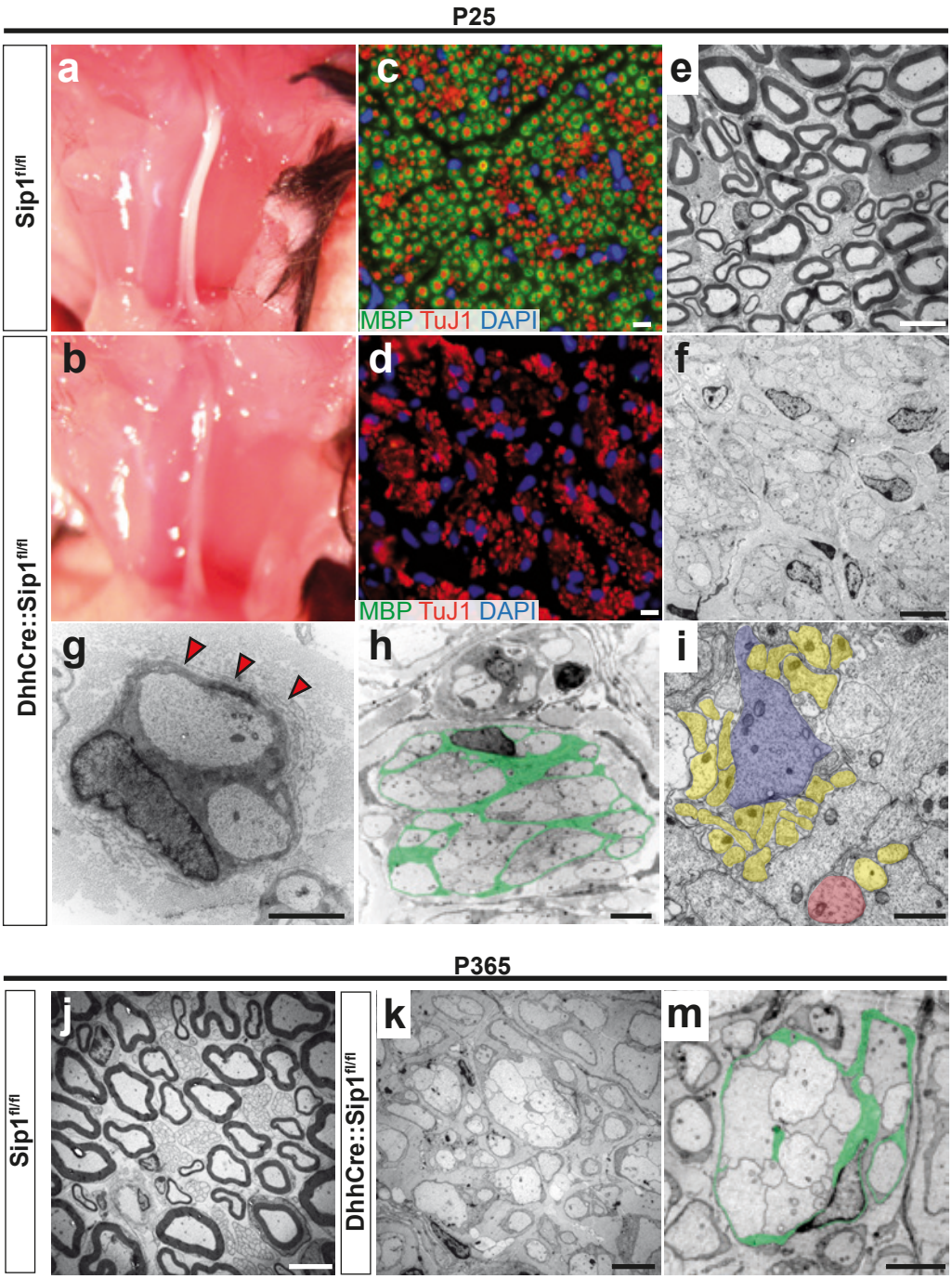

Figure 2. Mice lacking Sip1 in Schwann cells develop a severe neuropathy. Nerves of DhhCre::Sip1$^{fl/fl}$ mice appeared translucent (b) compared to controls (a) and did not show any myelin basic protein (MBP) staining at age P25 ((d), control in (c), MBP green, axons are stained in red by a class III beta-tubulin (TuJ1) antibody, representative images of n=3 animals per genotype). Axons in control nerves had been sorted and fully myelinated (e), while mutant nerves displayed large axon Schwann cell families and did not show any myelin ((f), representative images of n=5 animals per genotype). (g) Sip1-deficient Schwann cell engulfing two axons and displaying supernumerary loops of basal lamina (red arrow heads). (h) More than 50 axons surrounded by a single Schwann cell in the nerve of a conditional Sip1 mutant (Schwann cell cytoplasm false-coloured in green). (i) Axons belonging to one bundle varied in size as illustrated by false colours (small axons: yellow, medium sized axon: red, large axon: purple). (j-m) Dysmyelination and large axon-Schwann cell families persisted to the age of one year (P365) in nerves of conditional mutants ((j) control, (k) and (m) mutant). One bundle of axons from a nerve of a conditional mutant at age P365 is depicted in (m, Schwann cell cytoplasm false coloured in green). All images shown in g-m are representative of at least 3 animals per genotype and time point. Scale bars in all images 5 µm.

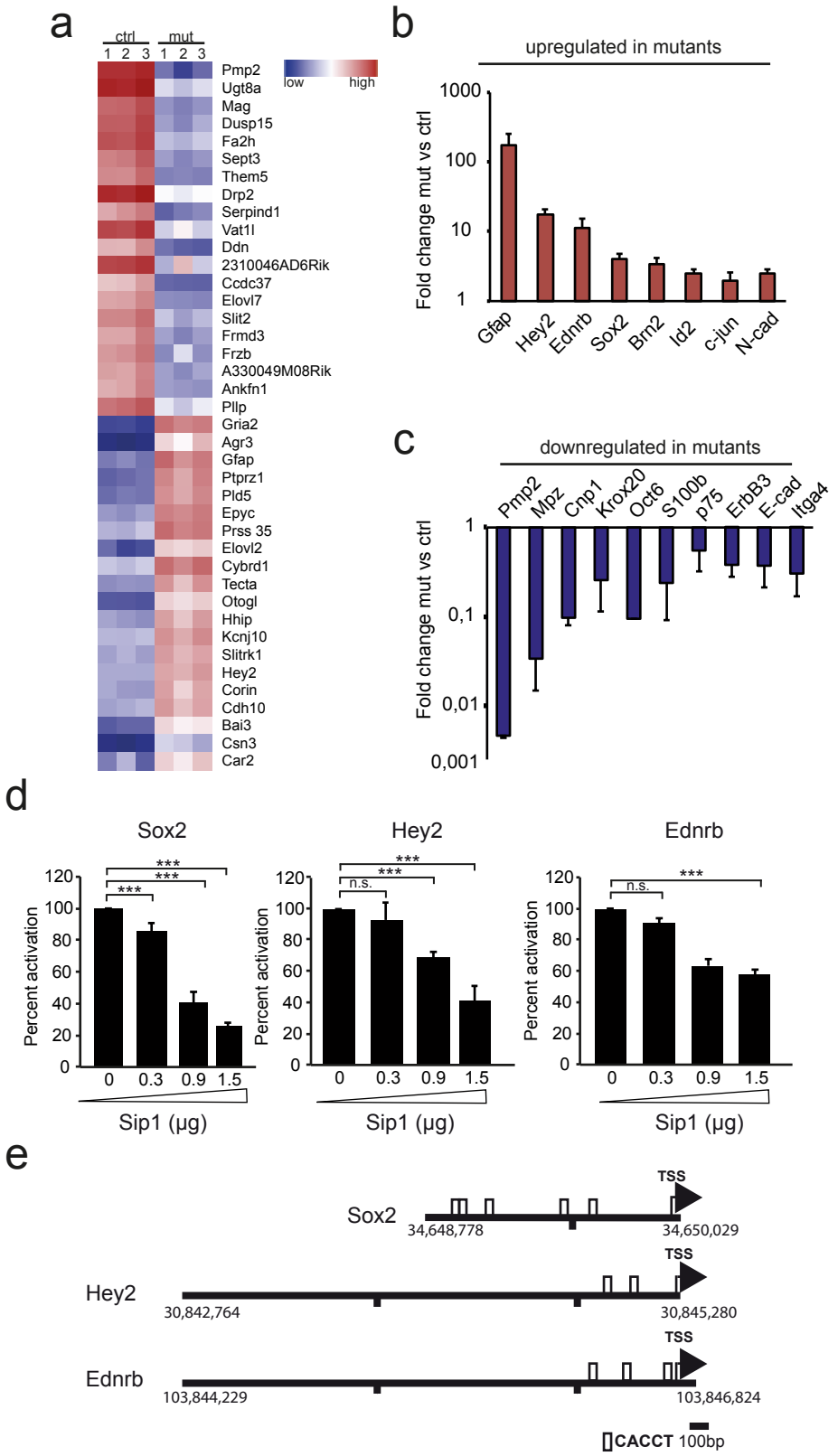

Figure 3. Sip1-deficient Schwann cells continuously express maturation inhibitors. (a) Heat map of a microarray analysis depicting the 20 most up- and downregulated genes in sciatic nerves of 3 DhhCre::Sip1$^{fl/fl}$ mice (mut) compared to those of 3 control littermates (ctrl) at age P25 (red: high expression, blue: low expression). A subset of promyelinating factors and maturation inhibitors were confirmed by quantitative realtime PCR ((b): upregulated genes; (c): downregulated genes, n=6 animals per genotype, bars depict mean values +/- SD, note the logarithmic scale). (d) Luciferase assays showing Sip1-dose-dependent diminished luciferase activity of Hey2, Ednrb and Sox2 promoter constructs upon cotransfection with a Sip1 expression plasmid (bars represent mean values of 3 independent experiments +/- SEM, activity of lysates from S16 cells co-transfected with the pGL2-luc plasmid containing the respective promoter fragment and the empty pCMV5 plasmid was considered 100%). (e) Scheme depicting the promoter fragments with predicted SIP1 binding sites used in (d). Numbers indicate location on the respective mouse chromosome.

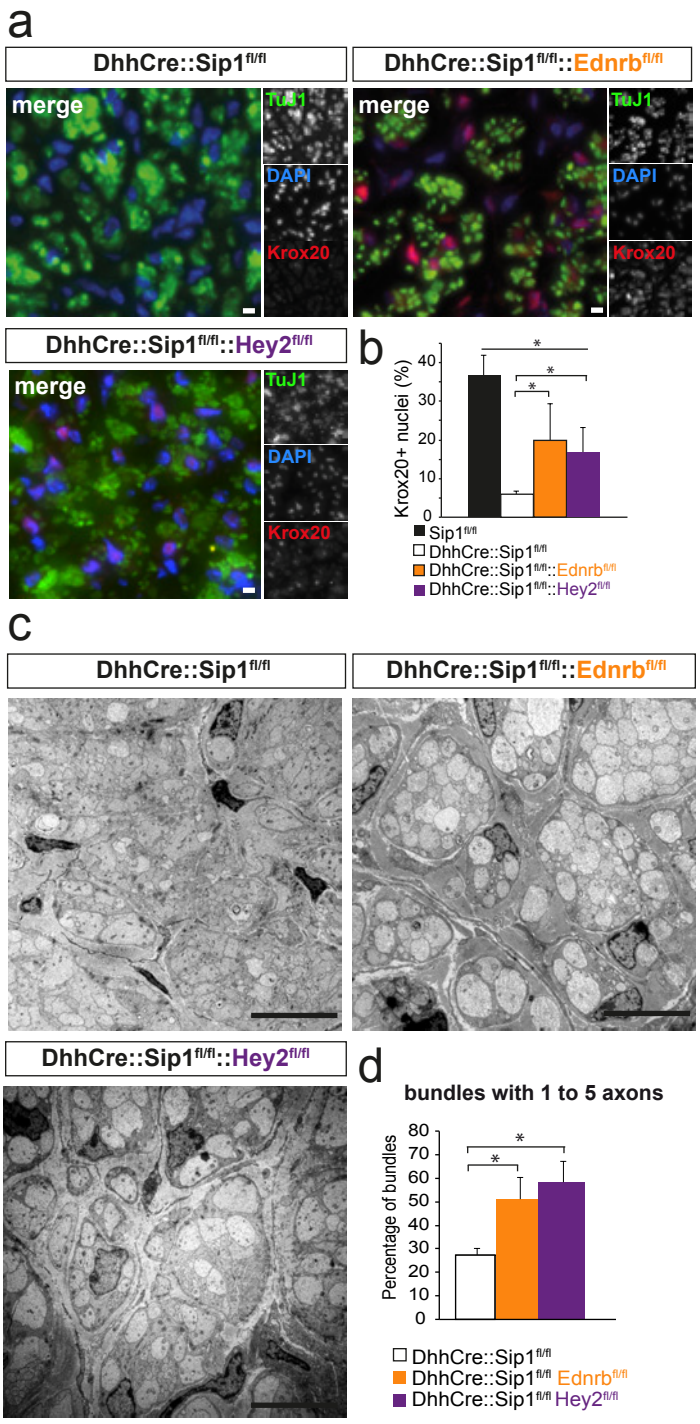

Figure 4. Sip1-mediated repression of Ednrb and Hey2 is functionally relevant in Schwann cells. (a) A subpopulation of Schwann cells in both Ednrb/Sip1 and Hey2/Sip1 conditional double mutants are KROX20-positive, while only few cells in Sip1 conditional mutants display a KROX20 signal (KROX20: red, class III beta-tubulin (TuJ1): green, DAPI: blue, representative images of n=5 animals per genotype, scale 5 µm). (b) Quantification of KROX20-positive nuclei (data are presented as mean values +/- SEM, n=5 animals per genotype, except $Sip1^{fl/fl}$ n=3 animals, $Sip1^{fl/fl}$ vs. $DhhCre::Sip1^{fl/fl}$ P=0.008, $DhhCre::Sip1^{fl/fl}$ vs. $DhhCre::Sip1^{fl/fl}::Ednrb^{fl/fl}$ P=0.03, $DhhCre::Sip1^{fl/fl}$ vs. $DhhCre::Sip1^{fl/fl}::Hey2^{fl/fl}$ P=0.019, $Sip1^{fl/fl}$ vs. $DhhCre::Sip1^{fl/fl}::Hey2^{fl/fl}$ P=0.004, $Sip1^{fl/fl}$ vs. $DhhCre::Sip1^{fl/fl}::Ednrb^{fl/fl}$ P=0.018, two-sided student's t-test of unpaired samples). (c) Improved radial sorting and smaller axon Schwann cell families in conditional double ($DhhCre::Sip1^{fl/fl}::Ednrb^{fl/fl}$ or $DhhCre::Sip1^{fl/fl}::Hey2^{fl/fl}$) compared to single ($DhhCre::Sip1^{fl/fl}$) mutants (representative images of 5 animals per genotype, scale 10 µm) at age P25. (d) Significantly higher number of axon-Schwann cell units with 1 to 5 axons per Schwann cell in both double mutant mice at age P25 compared to Sip1 single mutants (n=5 animals per genotype, at least 25 randomly chosen axon Schwann cell families per animal, mean values +/-SEM, $DhhCre::Sip1^{fl/fl}$ vs. $DhhCre::Sip1^{fl/fl}::Ednrb^{fl/fl}$ P=0.046, $DhhCre::Sip1^{fl/fl}$ vs. $DhhCre::Sip1^{fl/fl}::Hey2^{fl/fl}$ P=0.02, two-sided student's t-test of unpaired samples).

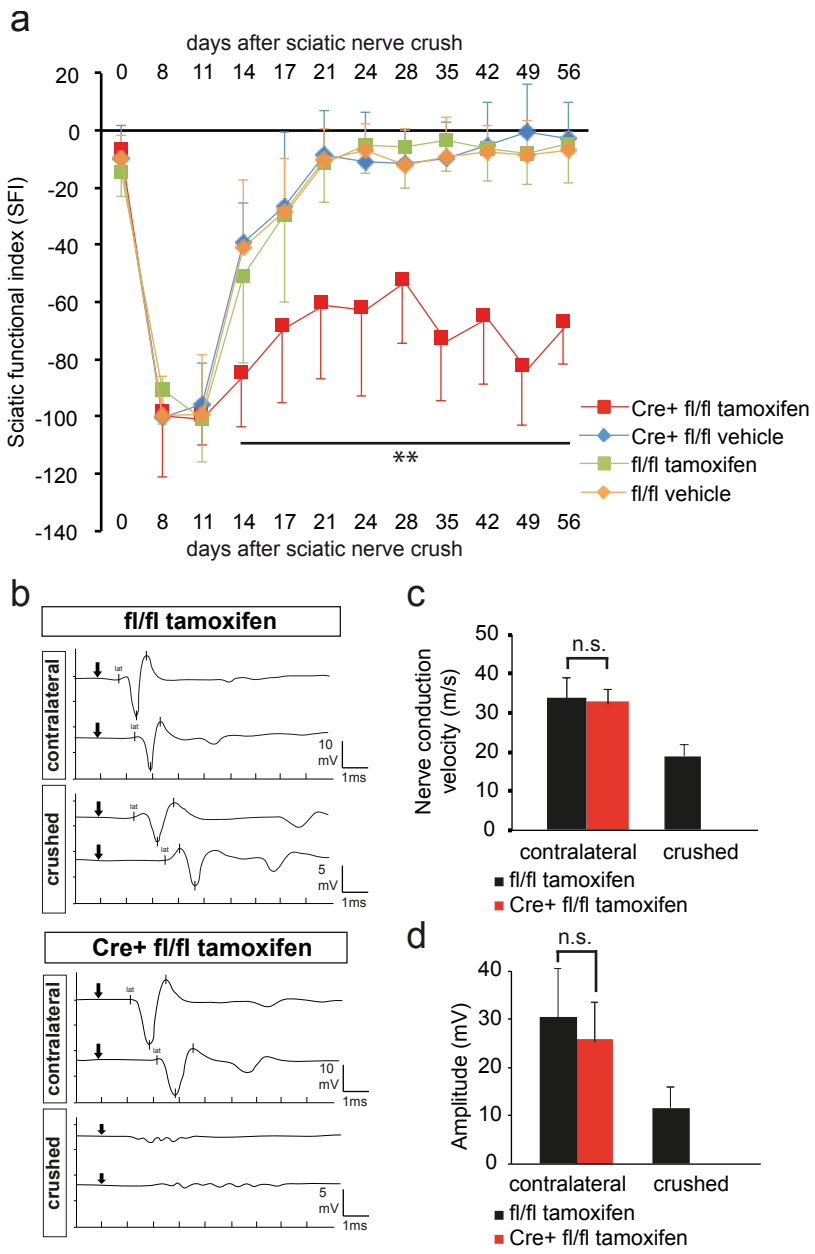

Figure 5. Sip1 is crucial for functional recovery after injury. (a) Functional recovery of tamoxifen-treated PLPCreERT2::Sip1$^{fl/fl}$ mice (Cre+ fl/fl tamoxifen) was significantly slower as determined by the sciatic functional index (SFI) compared to 3 control groups (n=10 animals per group and time point, mean values +/- SD). (b)-(d) Electrophysiological recordings after sciatic nerve stimulation 52 days after crush revealed a conduction block in tamoxifen-treated PLPCreERT2::Sip1$^{fl/fl}$ mice while control nerves had regained roughly 70% of the nerve conduction velocity of the contralateral unharmed nerve ((b) representative traces, (c) quantification of nerve conduction velocity, (d) distal amplitude, bars represent mean values +/- SD, n=8 animals Sip1$^{fl/fl}$ tamoxifen-treated, n=5 animals PLPCreERT2::Sip1$^{fl/fl}$ tamoxifen-treated).

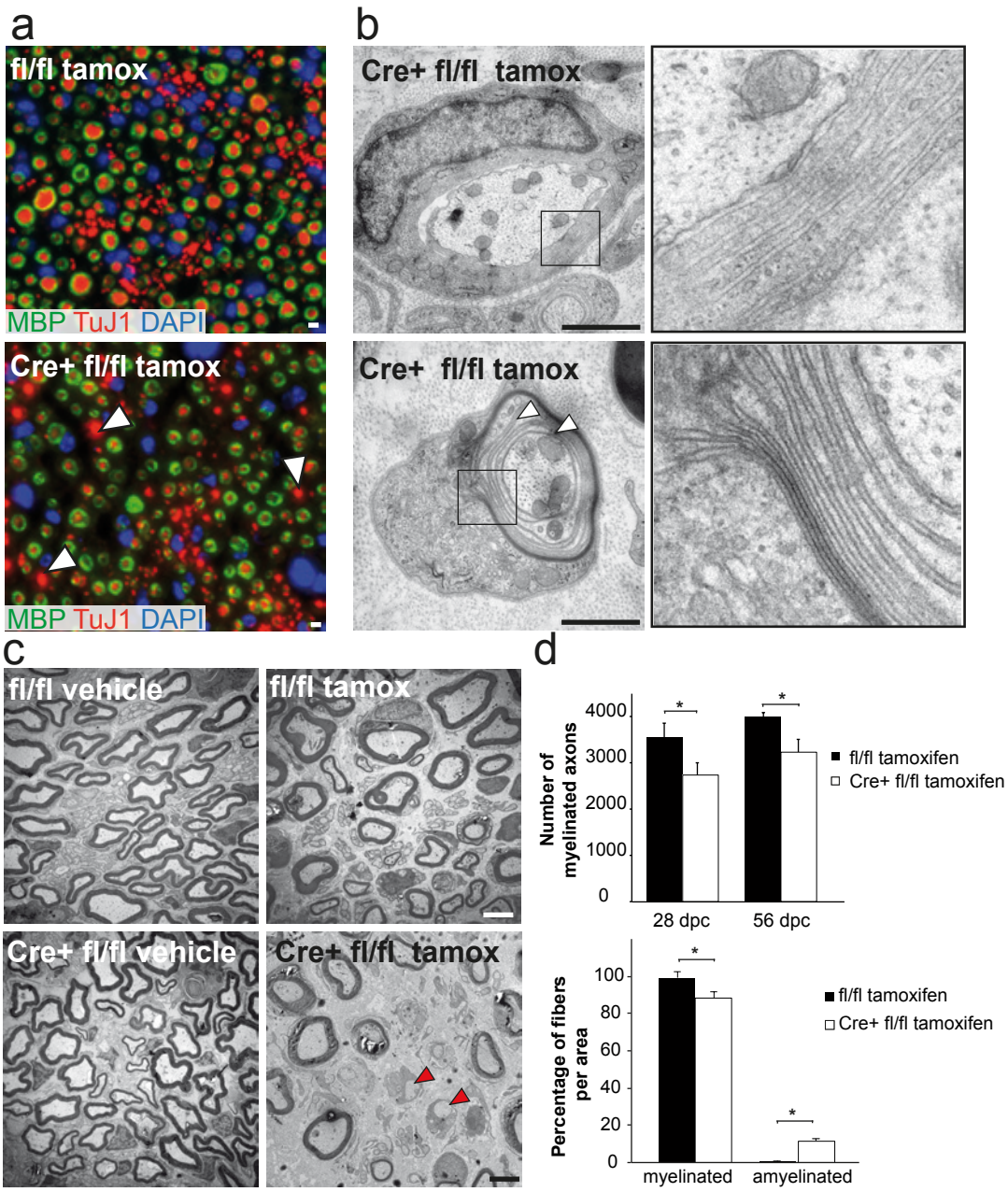

Figure 6. Remyelination by Sip1-deficient Schwann cells is impaired. (a) Immunohistochemistry for class III beta-tubulin (TuJ1, red) and MBP (green) on wax sections of sciatic nerves 56 days after crush showing large amyelinated fibers in tamoxifen-treated PLPCreERT2::Sip1$^{fl/fl}$ mice (Cre+ fl/fl tamox, representative images of 3 animals per group). (b) Ongoing remyelination in nerves of tamoxifen-treated PLPCreERT2::Sip1$^{fl/fl}$ mice 56 days after nerve crush evident by few non-compact myelin wraps as well as thin compact sheaths (scale 5 µm, boxed areas magnified in right panel). (c) Conditional mutants display fibrosis and large unmyelinated axons 56 days after crush (bottom right panel, red arrow heads, scale 5 µm). (d) There were significantly fewer remyelinated fibers in nerves of tamoxifen-treated PLPCreERT2::Sip1$^{fl/fl}$ mice 28 and 56 days after nerve crush (upper panel, bars represent mean values +/- SD, Sip1$^{fl/fl}$ tamoxifen-treated n=3, PLPCreERT2::Sip1$^{fl/fl}$ tamoxifen-treated n=4, 28 days P=0.023, 56 days P=0.0078, two-tailed student's t-test of unpaired samples) and roughly 11% of axons had remained amyelinated 56 days after crush (lower panel, bars represent mean values +/- SD, Sip1$^{fl/fl}$ tamoxifen-treated n=3, PLPCreERT2::Sip1$^{fl/fl}$ tamoxifen-treated n=4, myelinated P=0.036, amyelinated P=0.027, two-tailed student's t-test of unpaired samples).

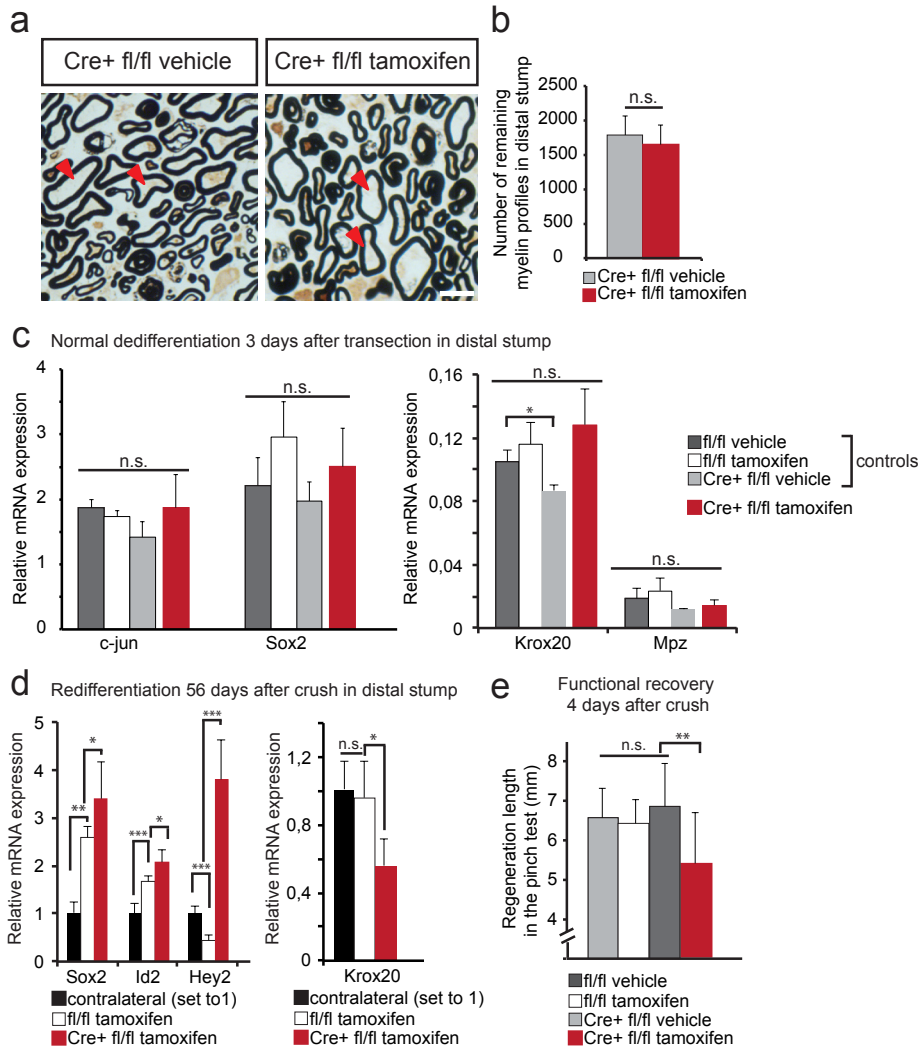

Figure 7. Impaired redifferentiation of Sip1-deficient Schwann cells. (a) and (b) Unaltered number of remaining myelin profiles in tamoxifen-treated PLPCreERT2:Sip1$^{fl/fl}$ mice (red arrow heads, right panel) compared to controls (red arrow heads, left panel) shown by silver impregnation of the distal sciatic nerve stump 3 days after transection (scale in (a) 10 µm, n=3 mice per group, bars in (b) represent mean values +/- SD, student's t-test for unpaired samples, P=0.50). (c) Comparable steady-state levels of mRNAs for c-jun and Sox2 in distal stumps of sciatic nerves of PLPCreERT2::Sip1$^{fl/fl}$ mice and controls 3 days after transection. Krox20 and Mpz mRNAs were drastically downregulated in mutants and the different control groups (expression in the contralateral unharmed nerve was set to 1, bars represent mean values +/- SD). (d) Increased levels of Sox2, Id2 and Hey2 mRNAs in tamoxifen-treated PLPCreERT2::Sip1$^{fl/fl}$ mice 56 days after nerve crush compared to controls. Krox20 levels remained low in nerves of mutants (bars represent mean values +/- SD, n=6 mice Cre+ fl/fl tamoxifen, n=5 mice fl/fl tamoxifen, n=5 mice contralateral). (e) Delayed early axon regrowth in tamoxifen-treated PLPCreERT2::Sip1$^{fl/fl}$ mice compared to controls 4 days after nerve crush as assessed by the pinch test (bars depict mean values +/- SD, n=13 mice per group except for fl/fl tamoxifen n=16, fl/fl Cre+ tamoxifen versus fl/fl Cre+ vehicle P=0.006, fl/fl Cre+ tamoxifen versus fl/fl tamoxifen P=0.0011, fl/fl Cre+ tamoxifen versus fl/fl vehicle P=0.0027, student's t-test of unpaired samples).

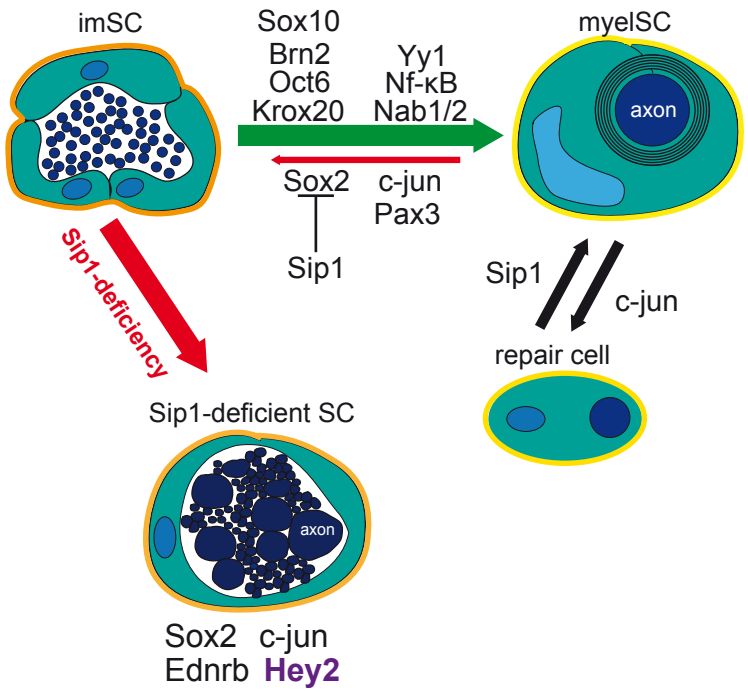

Figure 8. Hypothetical working model of Sip1 function in Schwann cells (adapted from Jessen and Mirsky, 2005). The development of immature Schwann cells (imSC, immature basal lamina depicted in orange) to mature myelinating Schwann cells (myelSC, mature basal lamina yellow) is driven by positive transcriptional regulators (green arrow). In parallel, suppressors of maturation (red arrow) need to be silenced. This is achieved by SIP1 acting as an “inhibitor of inhibition” thereby promoting differentiation. Sip1-inactivation in the Schwann cell lineage (Sip1-deficient SC, altered basal lamina light orange) leads to continous expression of differentiation inhibitors, such as Sox2, c-jun and Ednrb, and aberrant expression of the transcriptional repressor Hey2. At the same time, mRNA levels of Oct6, Krox20 and the genes coding for myelin proteins are low compared to mature myelinating Schwann cells. After injury, c-jun drives generation of an active repair cell, while Sip1 is crucial for the redifferentiation to a remyelination-competent Schwann cell.

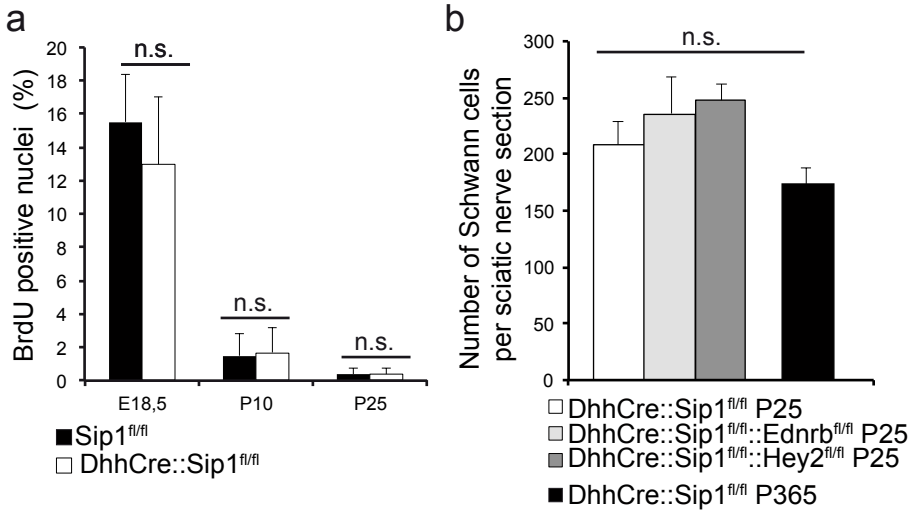

Supplementary Figure 1. Sip1-deficient Schwann cells survive and exit the cell cycle normally. (a) Unaltered levels of Schwann cell proliferation as detected by incorporation of Bromo-desoxyuridine (BrdU) in DhhCre::Sip1$^{fl/fl}$ mice compared to controls at E18.5, P10 and P25. Values are expressed as the percentage of BrdU-positive cells of all DAPI-positive nuclei +/- SD. (b) The number of Schwann cell nuclei per cross section of sciatic nerve was unaltered between conditional single mutants (DhhCre::Sip1$^{fl/fl}$) and both double conditional strains (DhhCre::Sip1$^{fl/fl}$::Ednrb$^{fl/fl}$ and DhhCre::Sip1$^{fl/fl}$::Hey2$^{fl/fl}$) at age P25. Additionally, the Schwann cell number of DhhCre::Sip1$^{fl/fl}$ mice at age P365 was unaltered compared to P25 (n=3 animals per age and genotype, all bars depict mean values +/- SD).

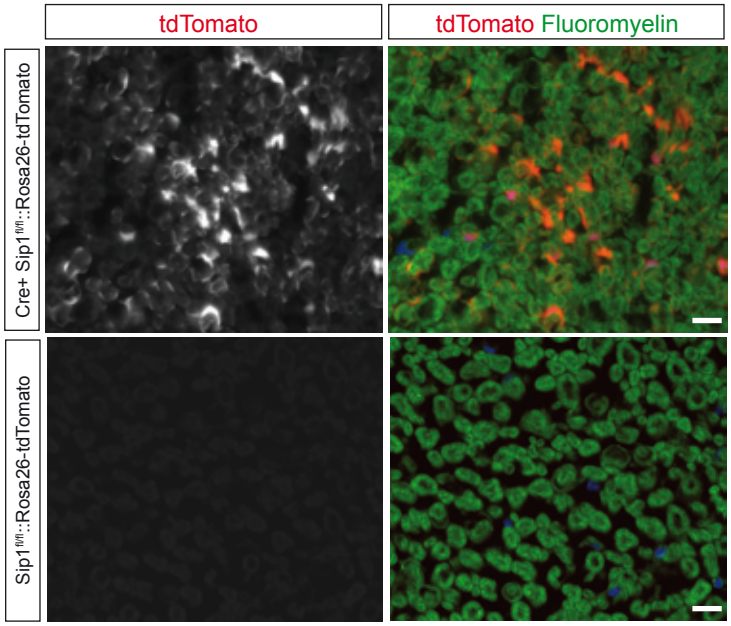

Supplementary Figure 2. Confirmation of recombination 4 weeks after the last tamoxifen-injection. 4 weeks after the last injection, endogenous tdTomato fluorescence (red) was observed in sciatic nerve cross sections of tamoxifen-treated PLPCreERT2::Sip1$^{fl/fl}$ mice (top panel), but not in treated Sip1$^{fl/fl}$ mice (bottom panel, myelin/fluoromyelin in green, scale 10 µm, representative images from n=3 mice per genoytpe).

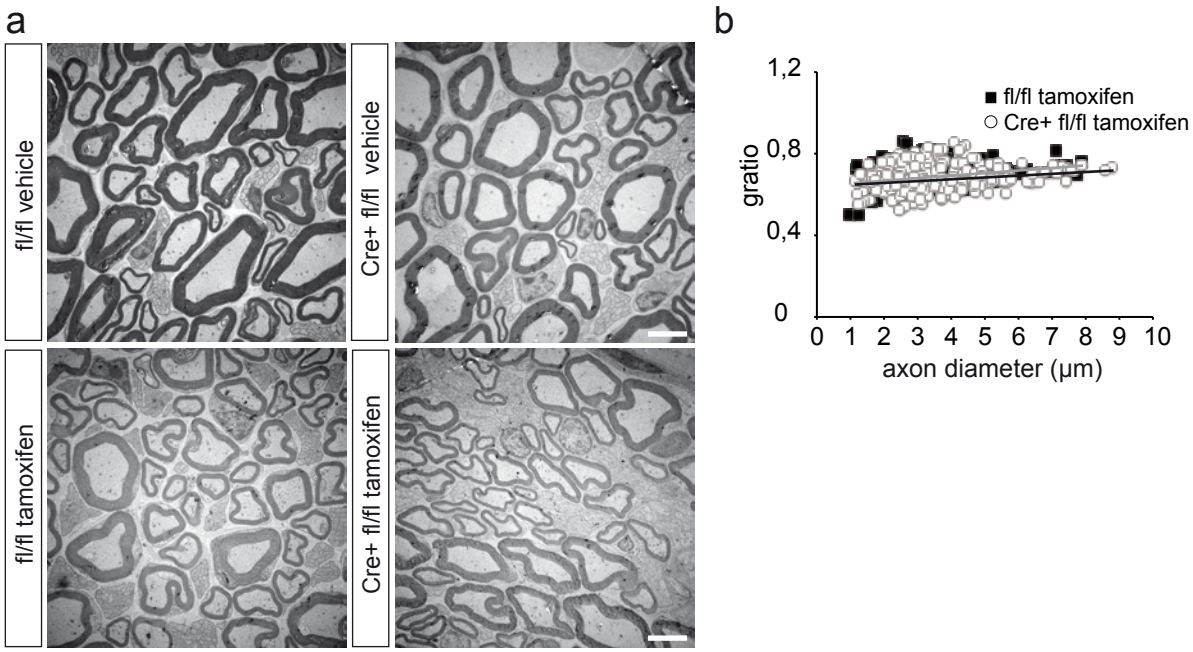

Supplementary Figure 3. Inactivation of Sip1 in adult mice. Myelin sheath thickness was unaltered 12 weeks after the last injection in tamoxifen-treated PLPCreERT2::Sip1$^{fl/fl}$ mice compared to the 3 respective control groups. Representative images are shown in (a), a scatter plot depicting the gratio in relation to the fiber diameter for tamoxifen-treated PLPCreERT2::Sip1$^{fl/fl}$ mice compared to tamoxifen-terated Sip1$^{fl/fl}$ mice in (b), (n=3 animals per group, at least 100 randomly chosen fibers per animal, scale in (a) 5 µm).

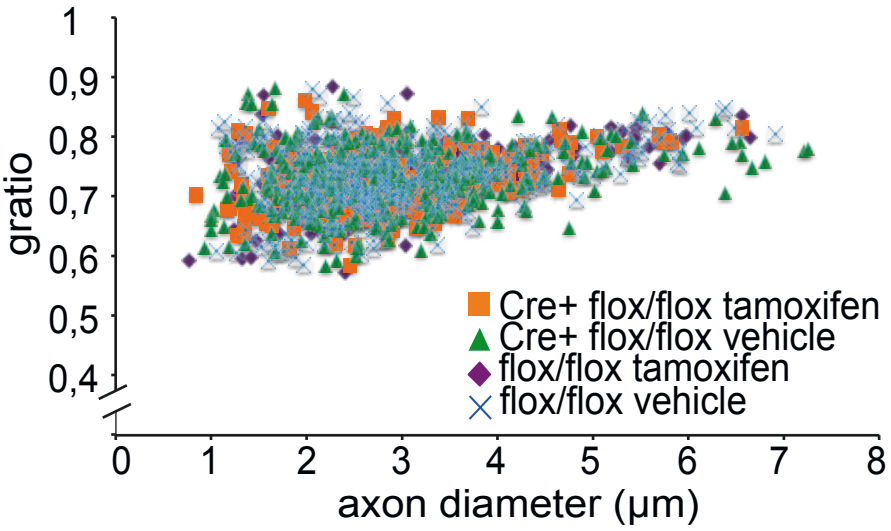

Supplementary Figure 4. Unaltered myelin sheath thickness after remyelination. Scatter plot depicting the gratio in relation to the fiber diameter of remyelinated fibers 8 weeks after nerve crush. No significant difference in myelin sheath thickness was observed between tamoxifen-treated PLPCreERT2::Sip1$^{fl/fl}$ mice and the 3 respective control groups (n=3 animals per group, at least 100 randomly chosen fibers per animal).